Biomagnetics: An Interdisciplinary Field Where Magnetics, Biology and Medicine Overlap

Shoogo Ueno

Professor Emeritus, The University of Tokyo
Professor, Graduate School of Engineering, Kyushu University
Dean, Faculty of Medical Technology, Teikyo University, Fukuoka

IEEE Magnetics Society

- **IEEE Magnetics Society Home Page: *www.ieeemagnetics.org***
  - 3000 full members
  - 300 student members

- **The Society**
  - Conference organization (INTERMAG, MMM, TMRC, etc.)
  - Student support for conferences
  - Large conference discounts for members
  - Local chapter activities
  - Distinguished lectures
  - Society awards

- ***IEEE Transactions on Magnetics***
  - ~2000 peer reviewed pages each year
  - Electronic access to all *IEEE Transactions on Magnetics* papers

- **New for 2010 *IEEE Magnetics Letters*;** a rapid-publication, primarily electronic, peer-reviewed journal dedicated exclusively to magnetics articles of substantial current interest. (See MagSoc Homepage)

- **Online applications for IEEE membership: *www.ieee.org/join***
  - 360,000 members
  - IEEE student membership ≈ $30
  - IEEE full membership ≈ $150

1. TMS (Transcranial Magnetic Stimulation)
2. MEG (Magnetoencephalography)
3. Impedance/Conductivity MRI and Current MRI
4. Cancer Therapy by Pulsed Magnetic Fields
5. Cell Orientation and Growth by Magnetic Fields
6. Ferritin and Iron Release/Uptake

William Gilbert, Father of Magnetism
"The Earth is itself a huge magnet."

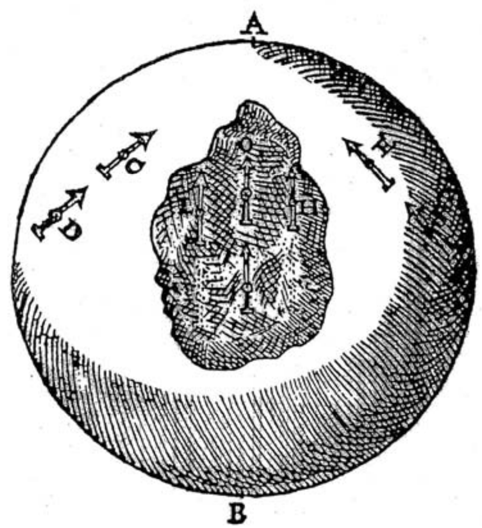

De Magnete, William Gilbert (1600)

"Magnetic force is animate or imitates life; and in many things surpasses human life, while this is bound up in the organic body."

-William Gilbert, 1600

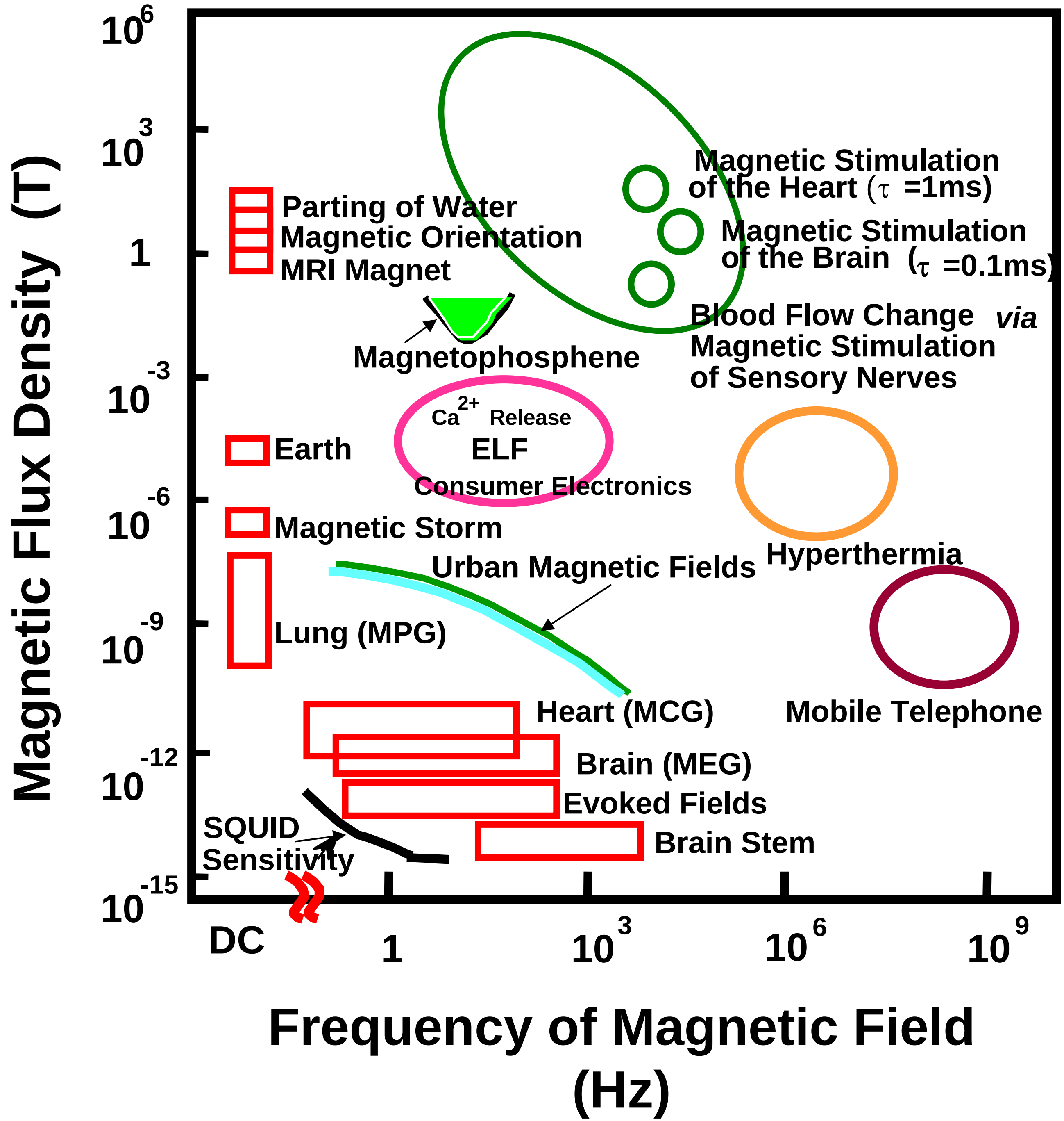

Magnetic Flux Density (T)
10^6
10^3
1
10^{-3}
10^{-6}
10^{-9}
10^{-12}
10^{-15}
Parting of Water
Magnetic Orientation
MRI Magnet
Magnetophosphene
Magnetic Stimulation of the Heart (τ =1ms)
Magnetic Stimulation of the Brain (τ =0.1ms)
Blood Flow Change *via* Magnetic Stimulation of Sensory Nerves
Ca^{2+} Release
ELF
Consumer Electronics
Earth
Magnetic Storm
Urban Magnetic Fields
Hyperthermia
Lung (MPG)
Mobile Telephone
Heart (MCG)
Brain (MEG)
Evoked Fields
Brain Stem
SQUID Sensitivity
DC
1
10^3
10^6
10^9
Frequency of Magnetic Field (Hz)

TMS（Transcranial Magnetic Stimulation)

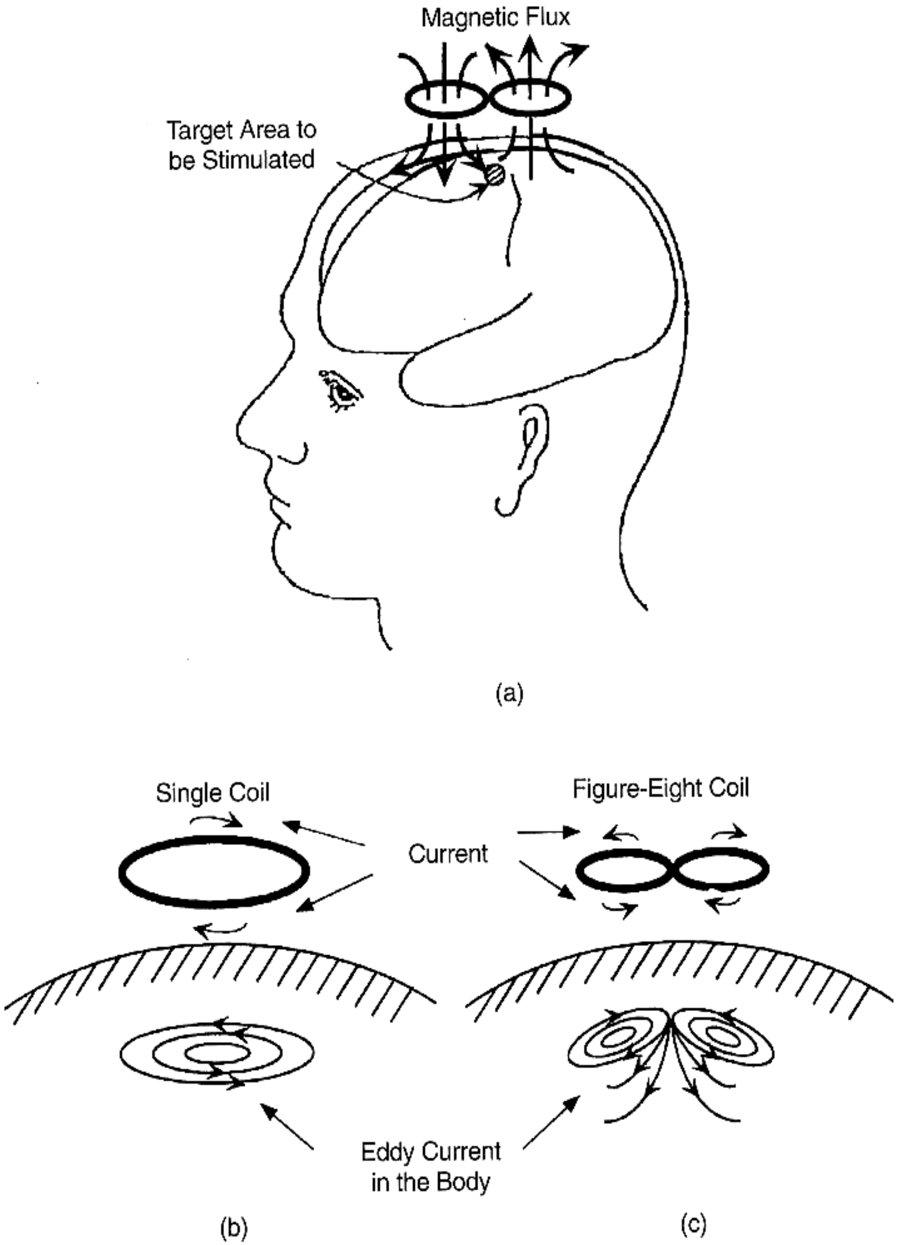

Current Distributions in TMS

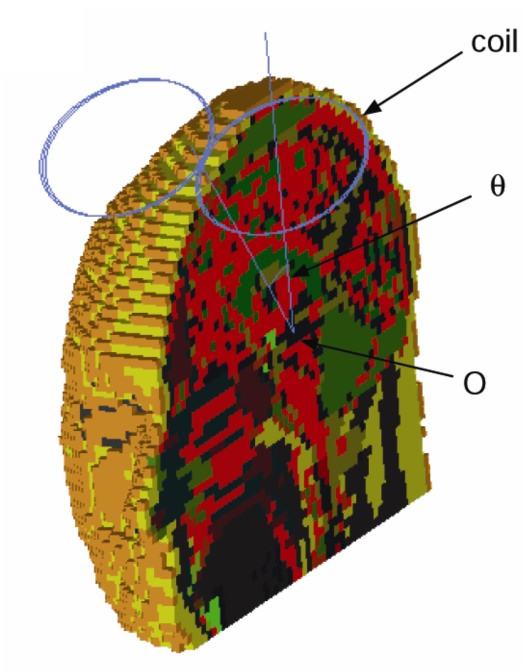

Numerical model of the human head

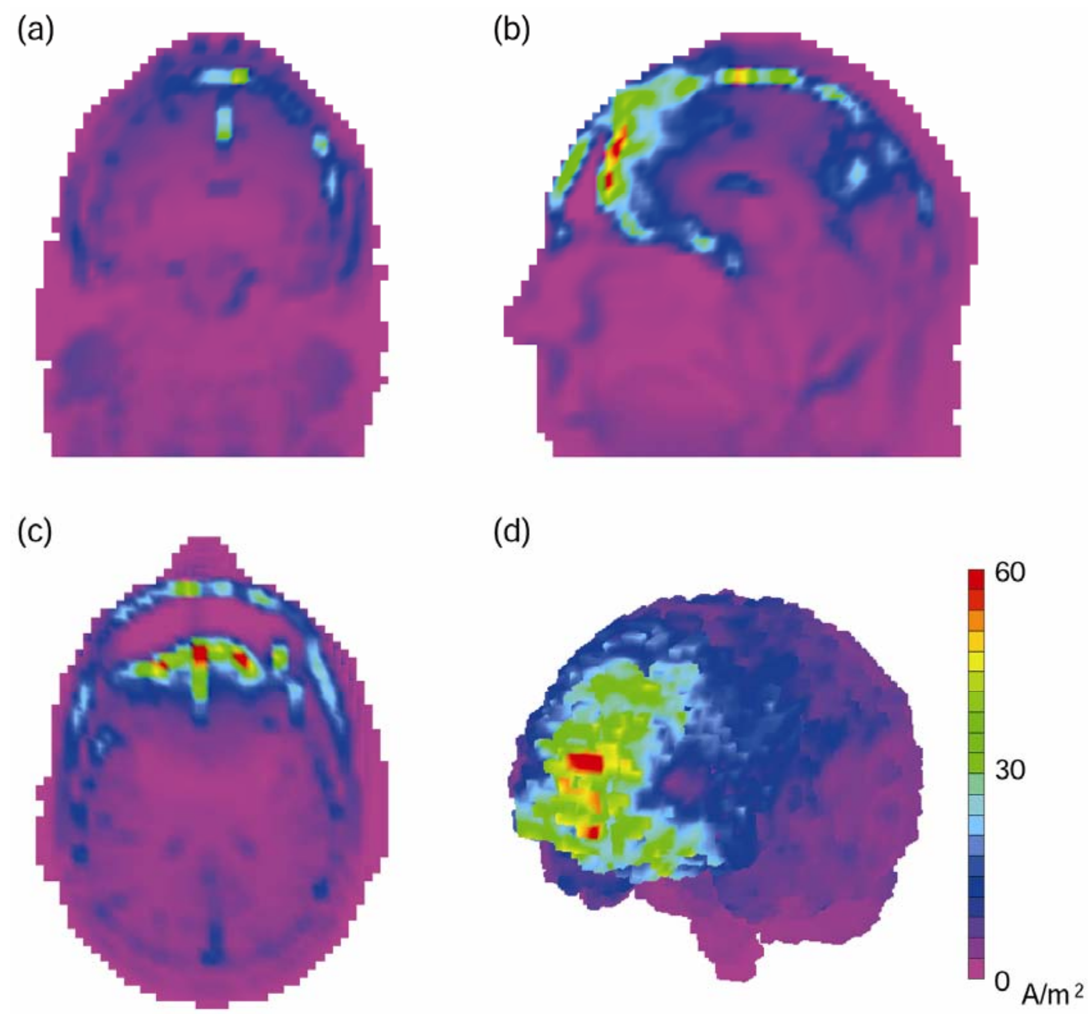

Current distributions in TMS represented in (a) coronal, (b) sagittal, and (c) transversal slices, and (d) the brain surface.

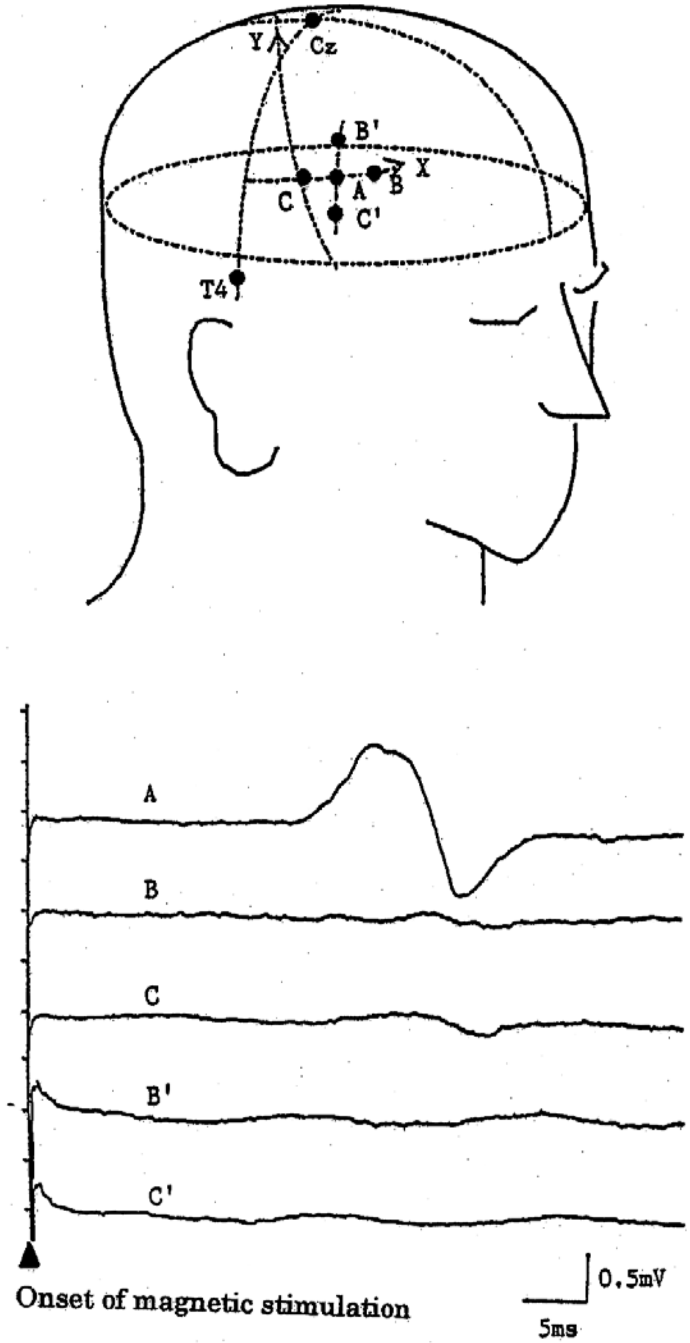

Y
Cz
B'
X
C
A
B
C'
T4
A
B
C
B'
C'
Onset of magnetic stimulation
0.5mV
5ms

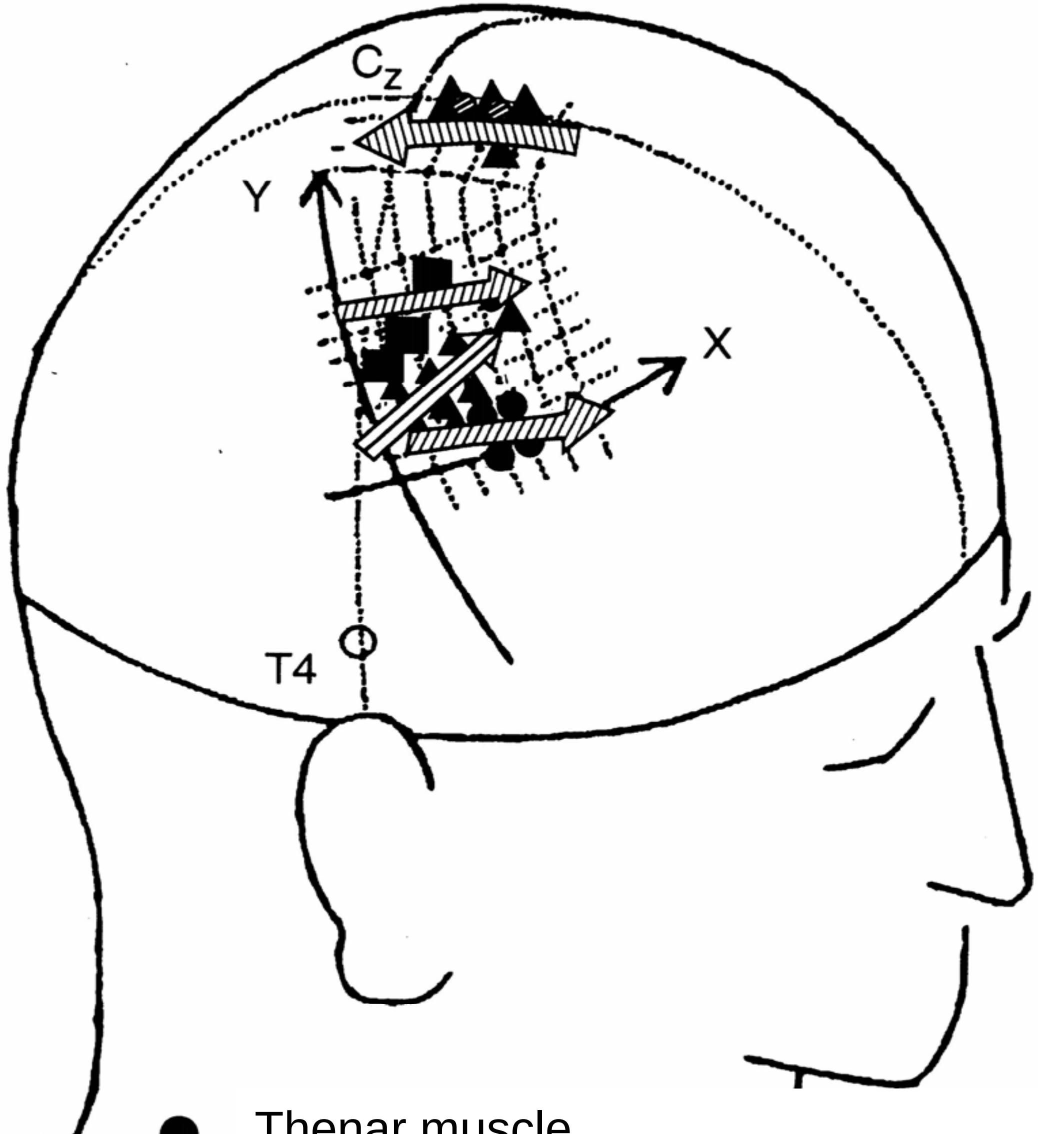

Cz
Y
X
T4

Thenar muscle
Hypothenar muscle
Bracioradial muscles
Abductor hallucis muscle
Abductor digiti minimi muscle

Medical Applications of Transcranial Magnetic Stimulation

1. Estimation of localized brain function

2. Creating virtual lesions to disturb dynamic neuronal connectivities

3. Damage prevention and regeneration of neurons

4. Modulation of neuronal plasticity

5. Therapeutic and diagnostic applications for the treatment of CNS diseases and mental illnesses

- Working memory is dependent on prefrontal granular cortex.
- Associative memory is dependent on the hippocampus and temporal lobe.

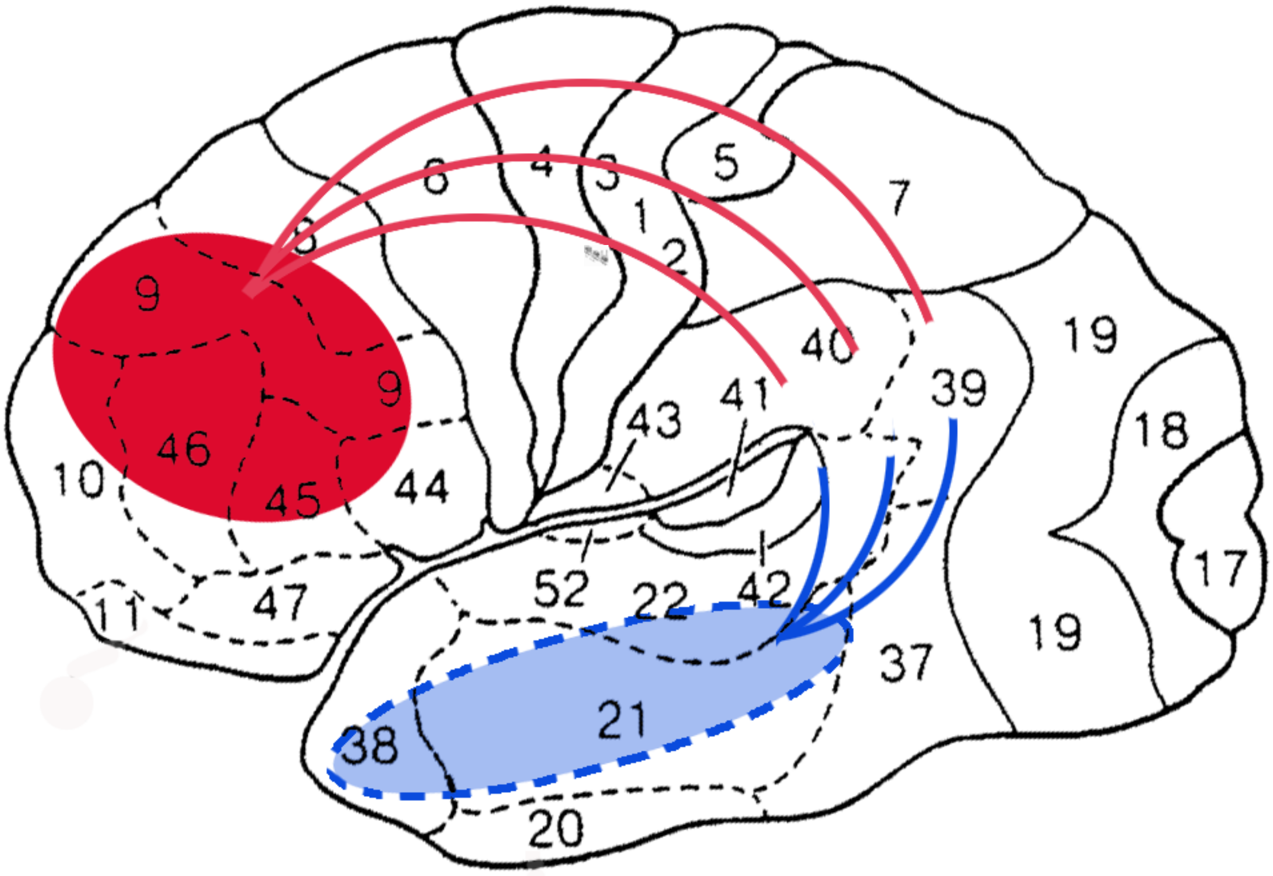

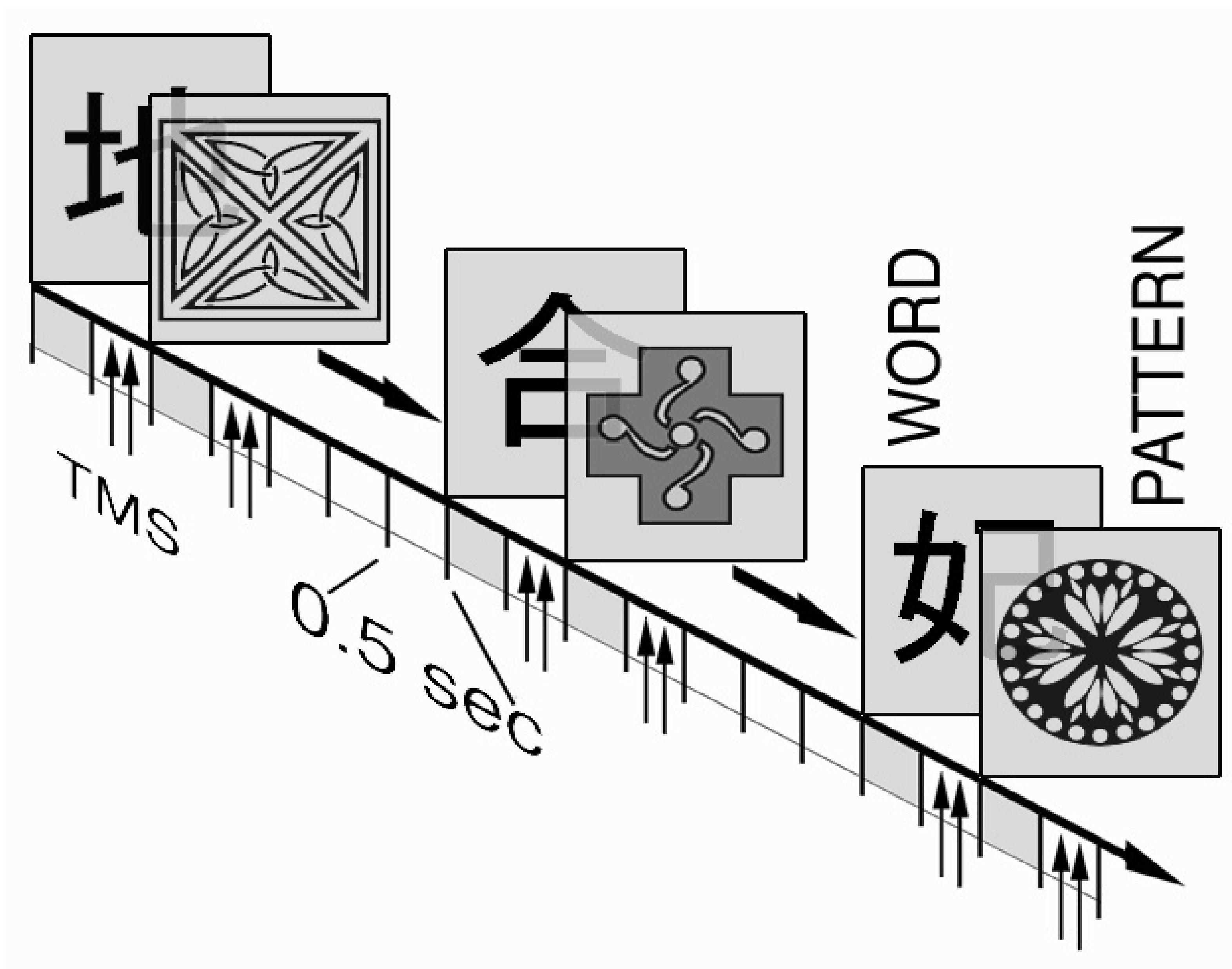

TMS
0.5 sec
WORD
PATTERN

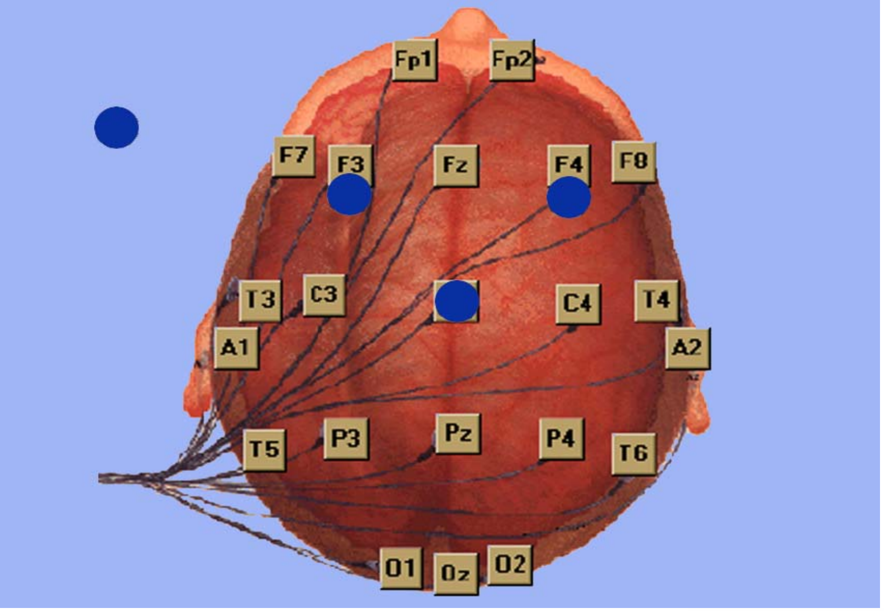
Fp1
Fp2
F7
F3
Fz
F4
F8
T3
C3
C4
T4
A1
A2
T5
P3
Pz
P4
T6
O1
Oz
O2

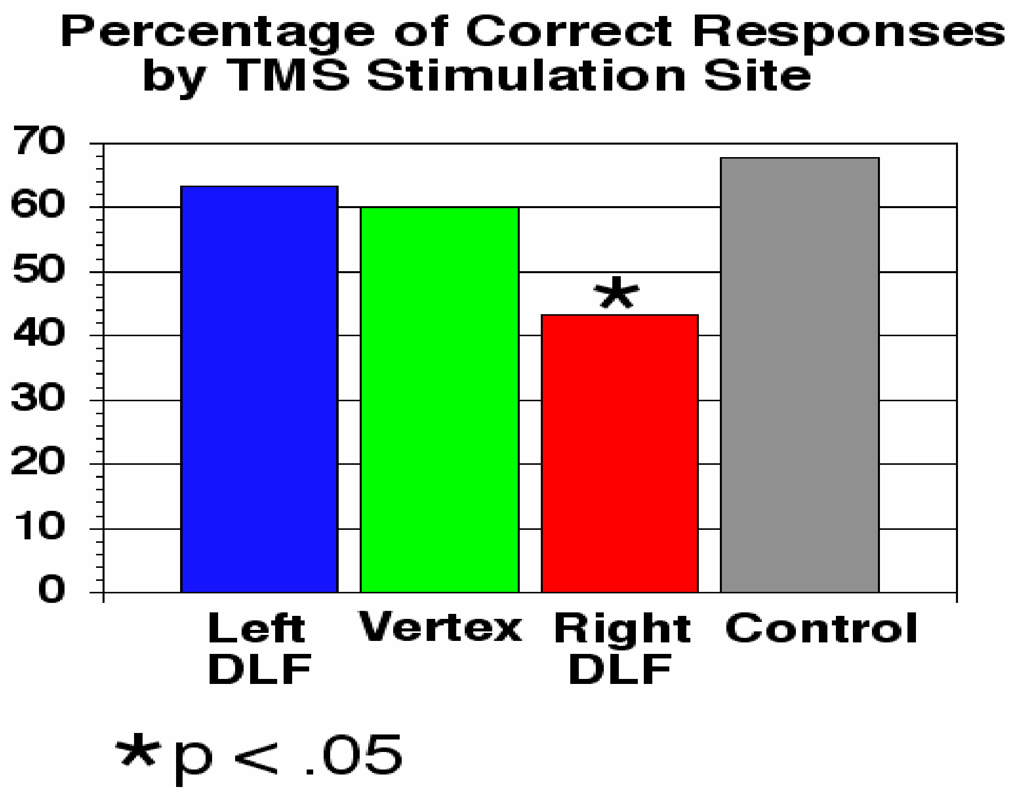
Percentage of Correct Responses by TMS Stimulation Site
70
60
50
40
30
20
10
0
*
Left DLF
Vertex
Right DLF
Control
*p < .05

Intra- and Interhemispheric Connectivity

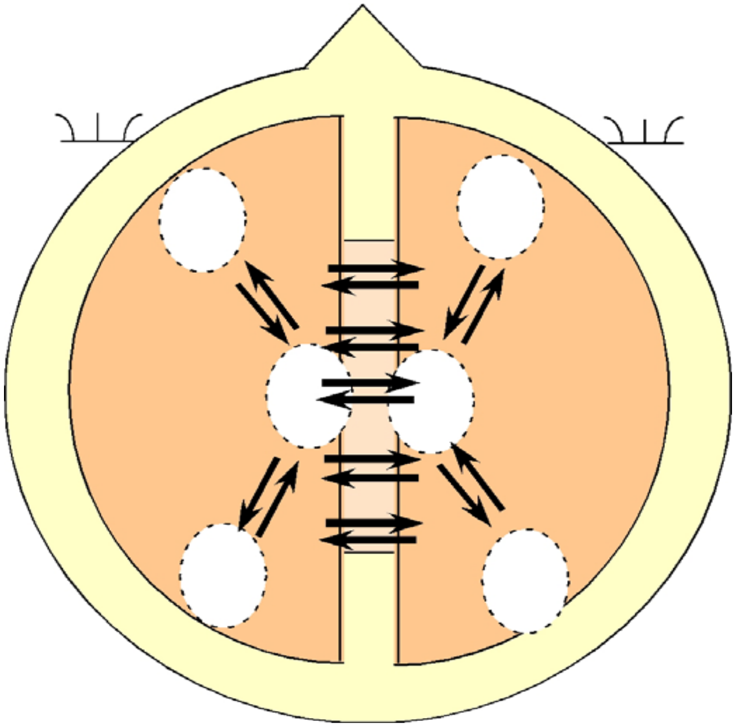

Interhemispheric connectivity

Commissural fibers

- **corpus callosum**
- **anterior/posterior commissure**
- **hippocampal commissure**

Method of stimulation

- A figure-of-eight 70mm coil was used (inner diameter: 53 mm, outer diameter: 73 mm)
- Direction of the induced current of TMS was from posterior to the anterior.
- Stimulus intensities were 70 % of motor threshold.

Scene of the experiment

EEG waveform

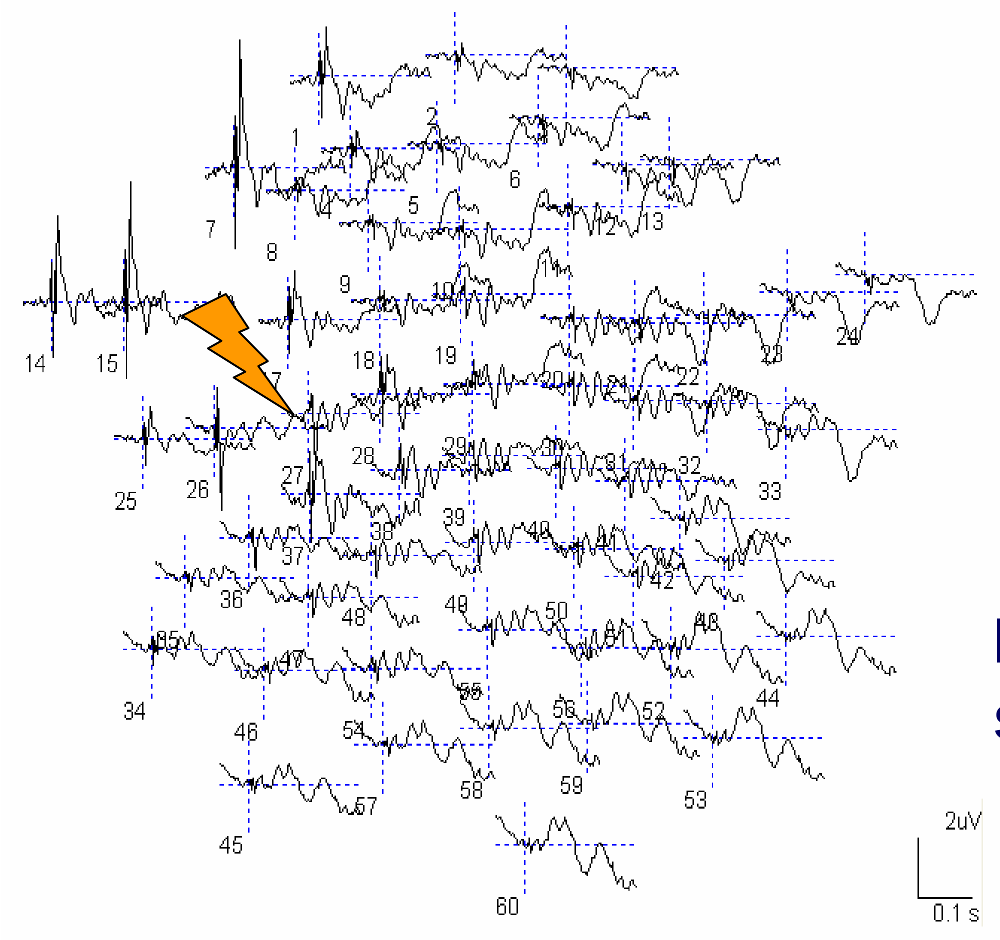

EEG when point A was stimulated.

EEG topography

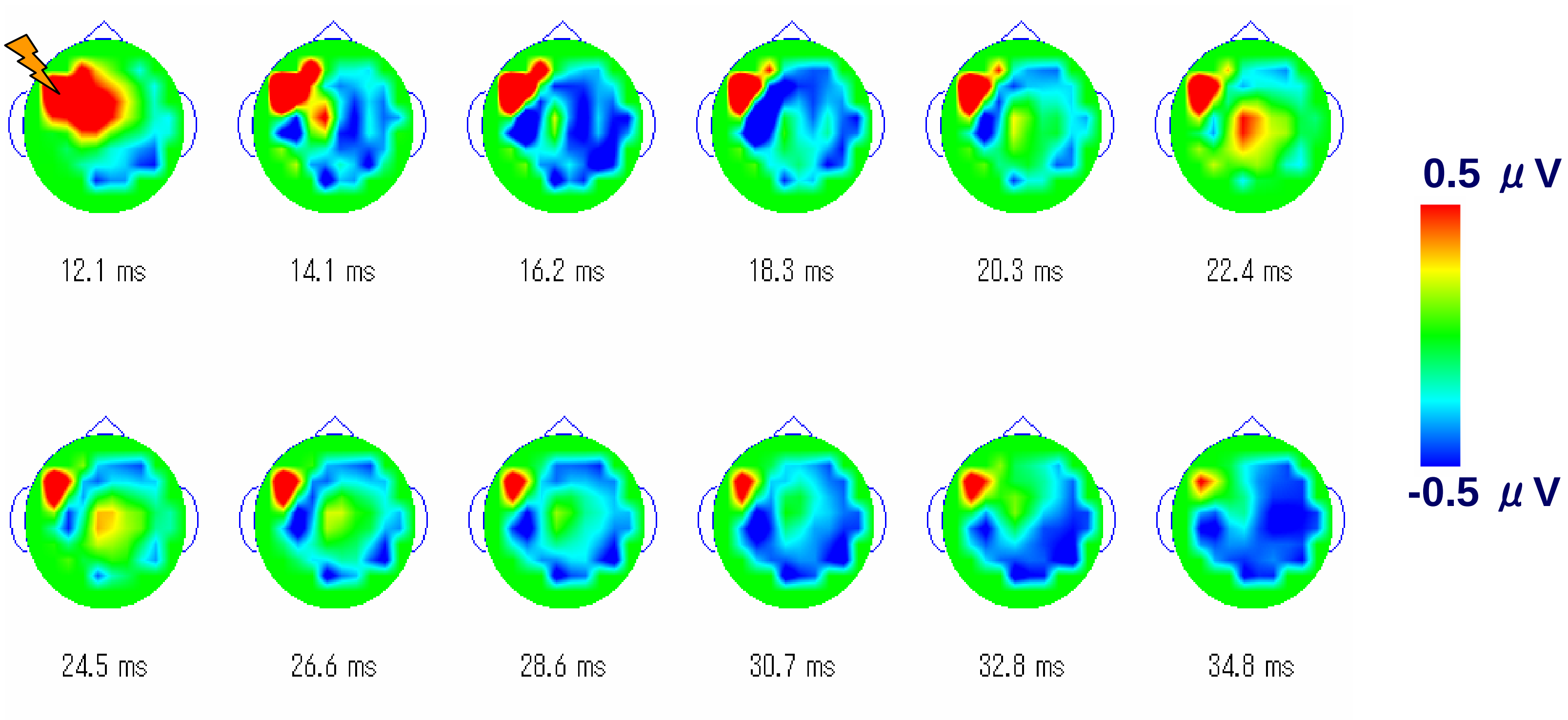

EEG topography when point A was stimulated.

EEG topography and Current distributions

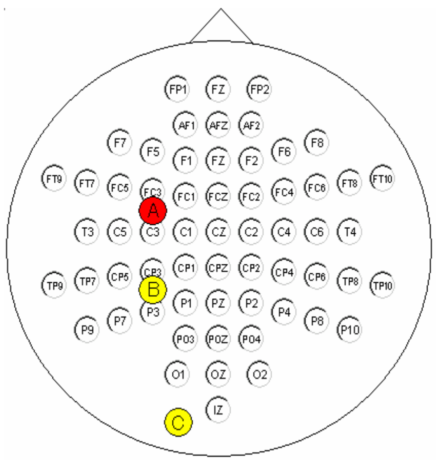

EEG topography

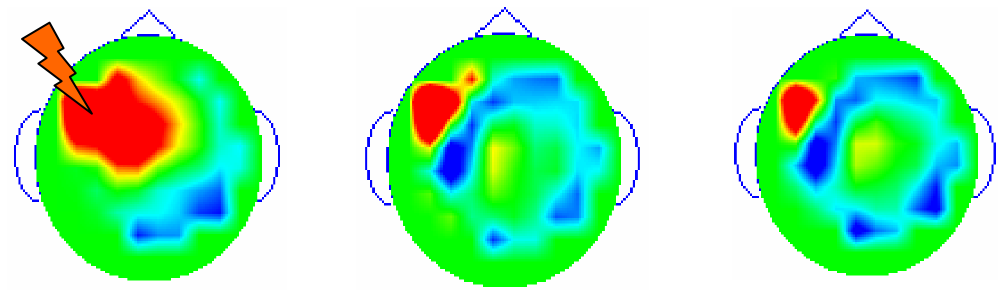

Current distribution

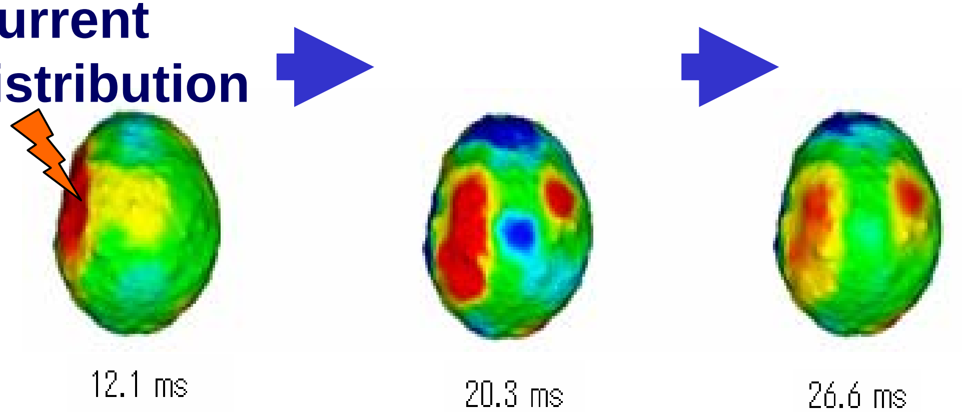

0.5 μV

0.1 mA/m^2

-0.5 μV

-0.1 mA/m^2

Current distribution when point A was stimulated

Long-term potentiation, LTP

Long-lasting increase in synaptic efficacy resulting from high-frequency stimulation of afferent fibers.

LTP in the hippocampus = typical morel of synaptic plasticity related to learning and memory.

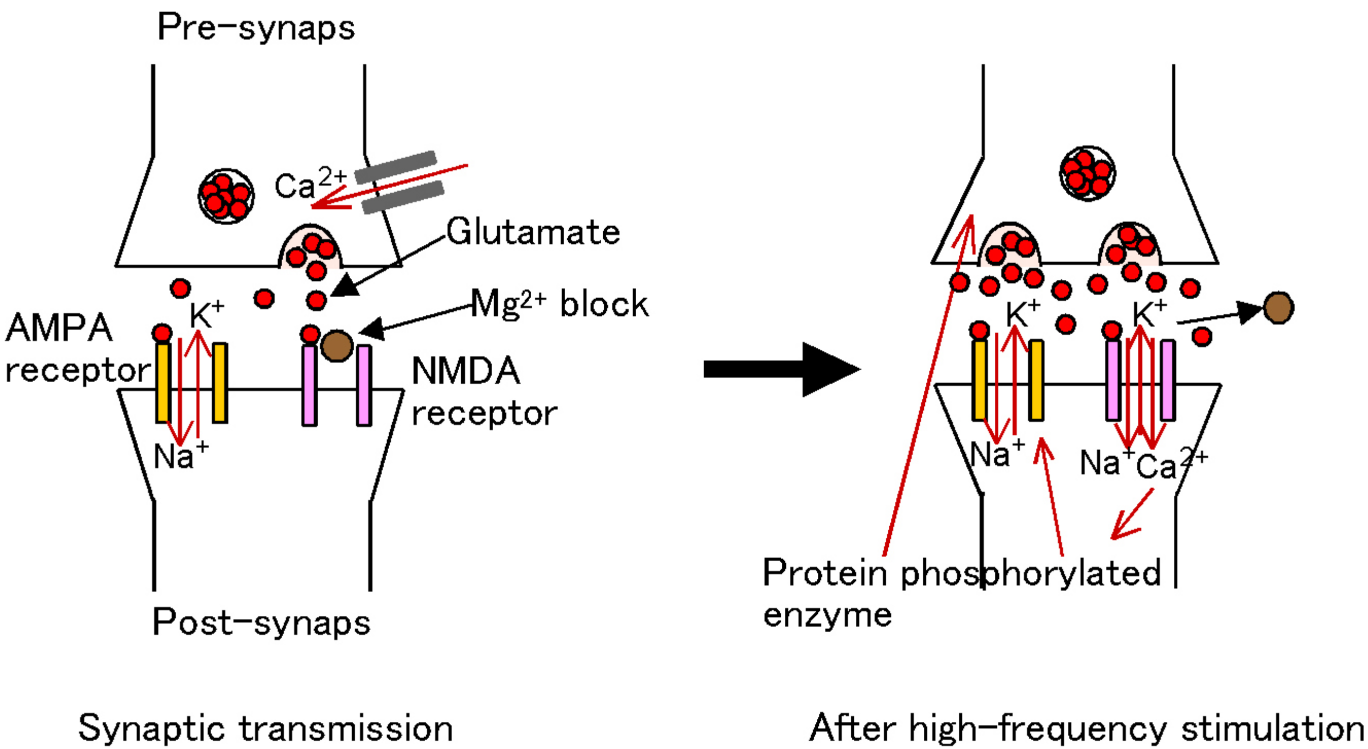

- Enhancement of transmitter release
- Activation of AMPA and NMDA receptors

Measurement of fEPSP and LTP

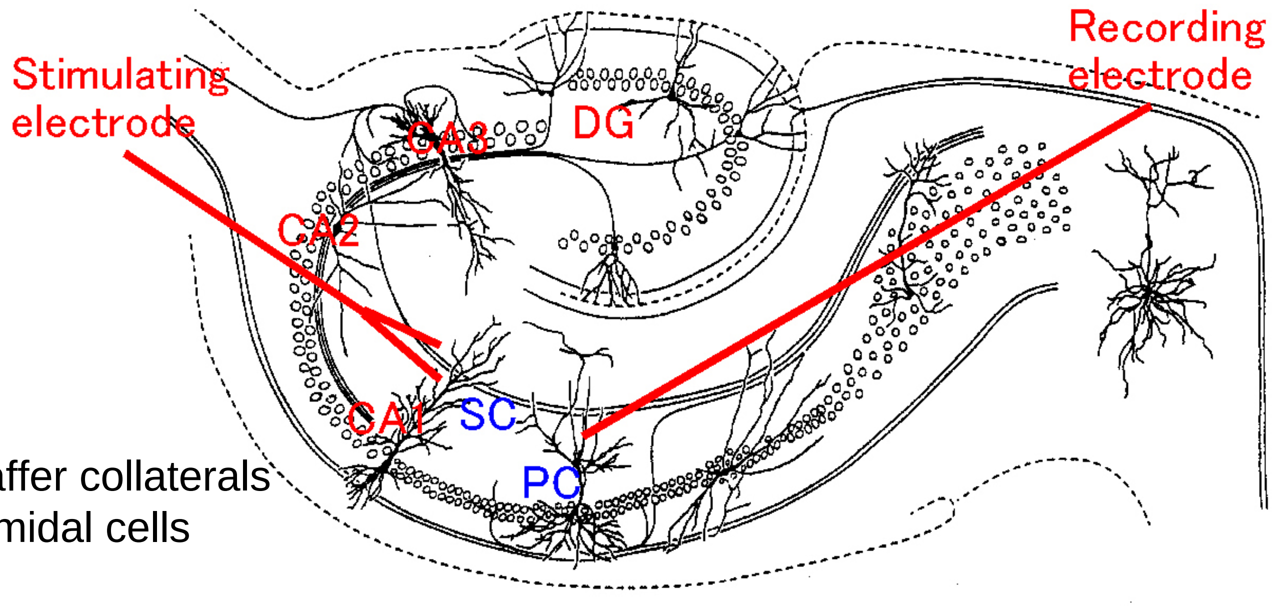

SC: Schaffer collaterals
PC: pyramidal cells

Excitatory postsynaptic potential (EPSP)

Tetanus stimulation (100 Hz for 1 sec) →Enhancement of EPSP
= Long-term potentiation (LTP)

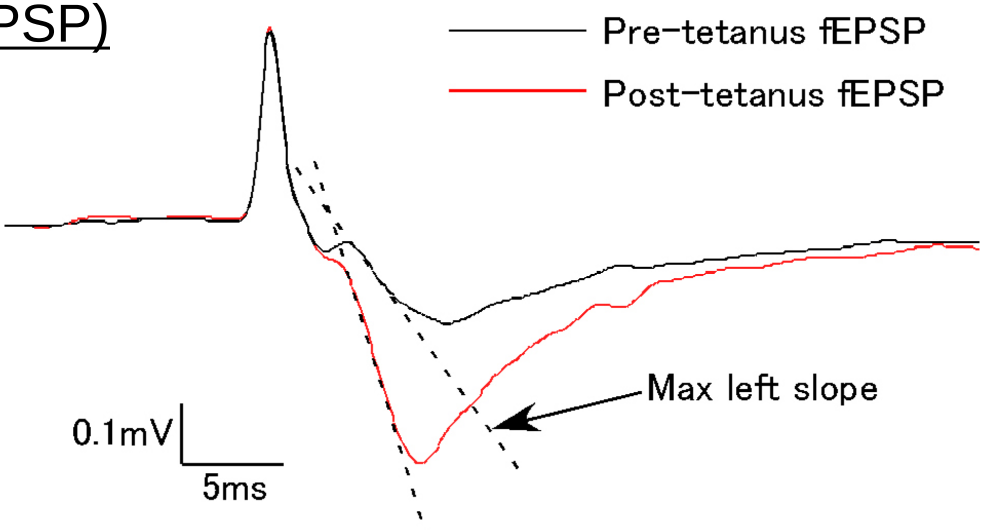

LTPs of 0.75 T TMS

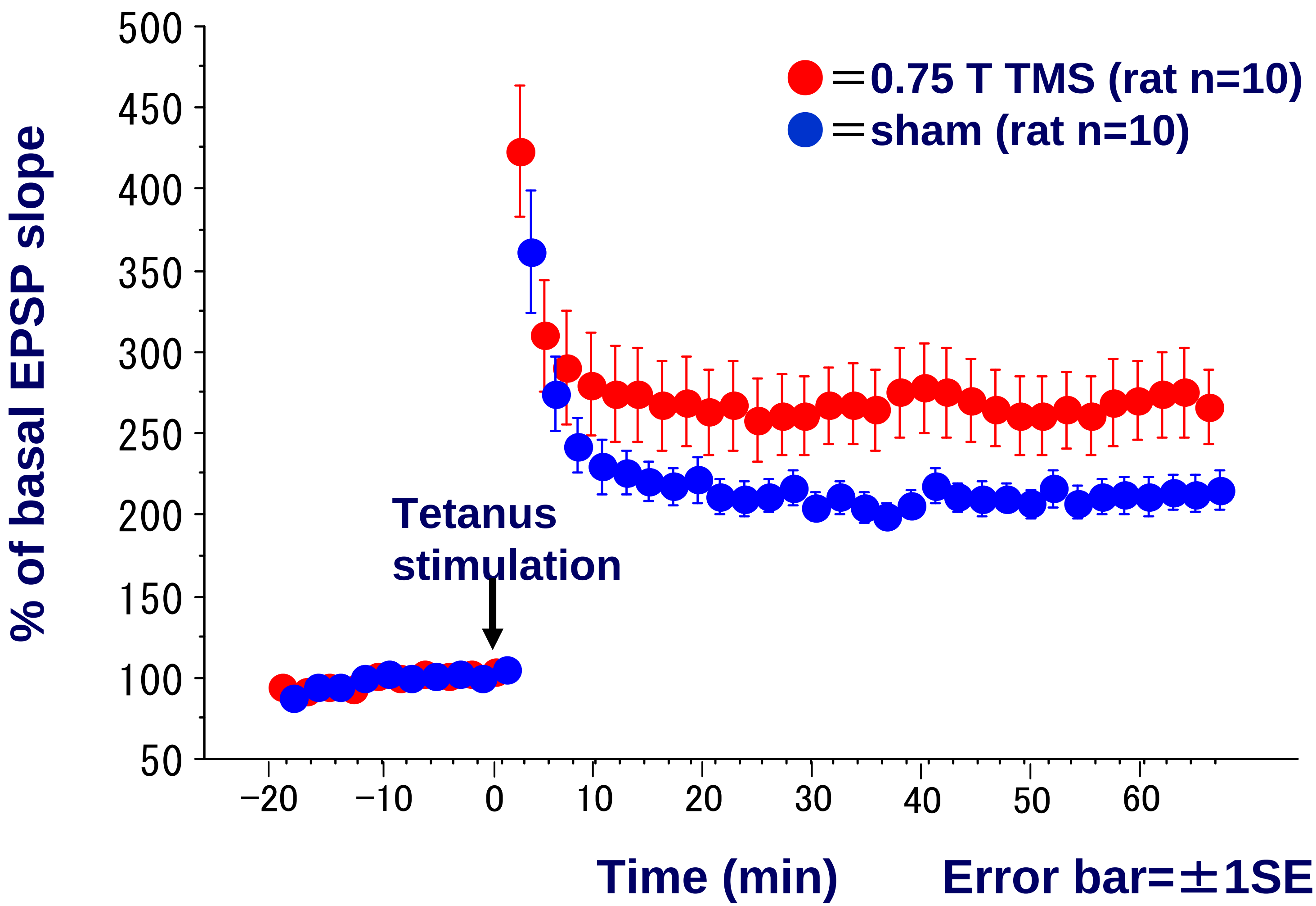

LTP of 0.75T TMS group was significantly enhanced (p=0.0408).

LTPs of 1.25 T TMS

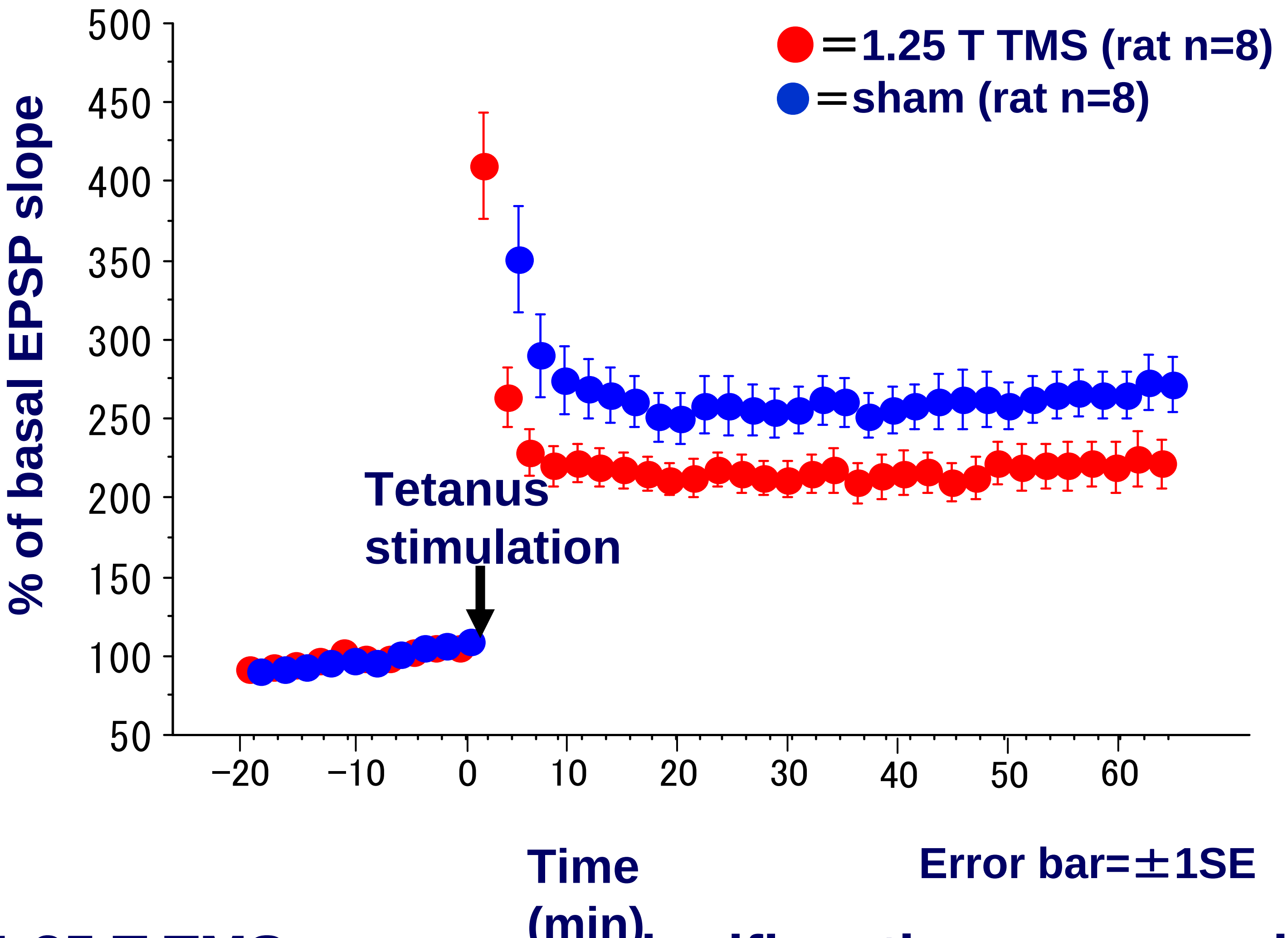

LTP of 1.25 T TMS group was significantly suppressed (p=0.0289).

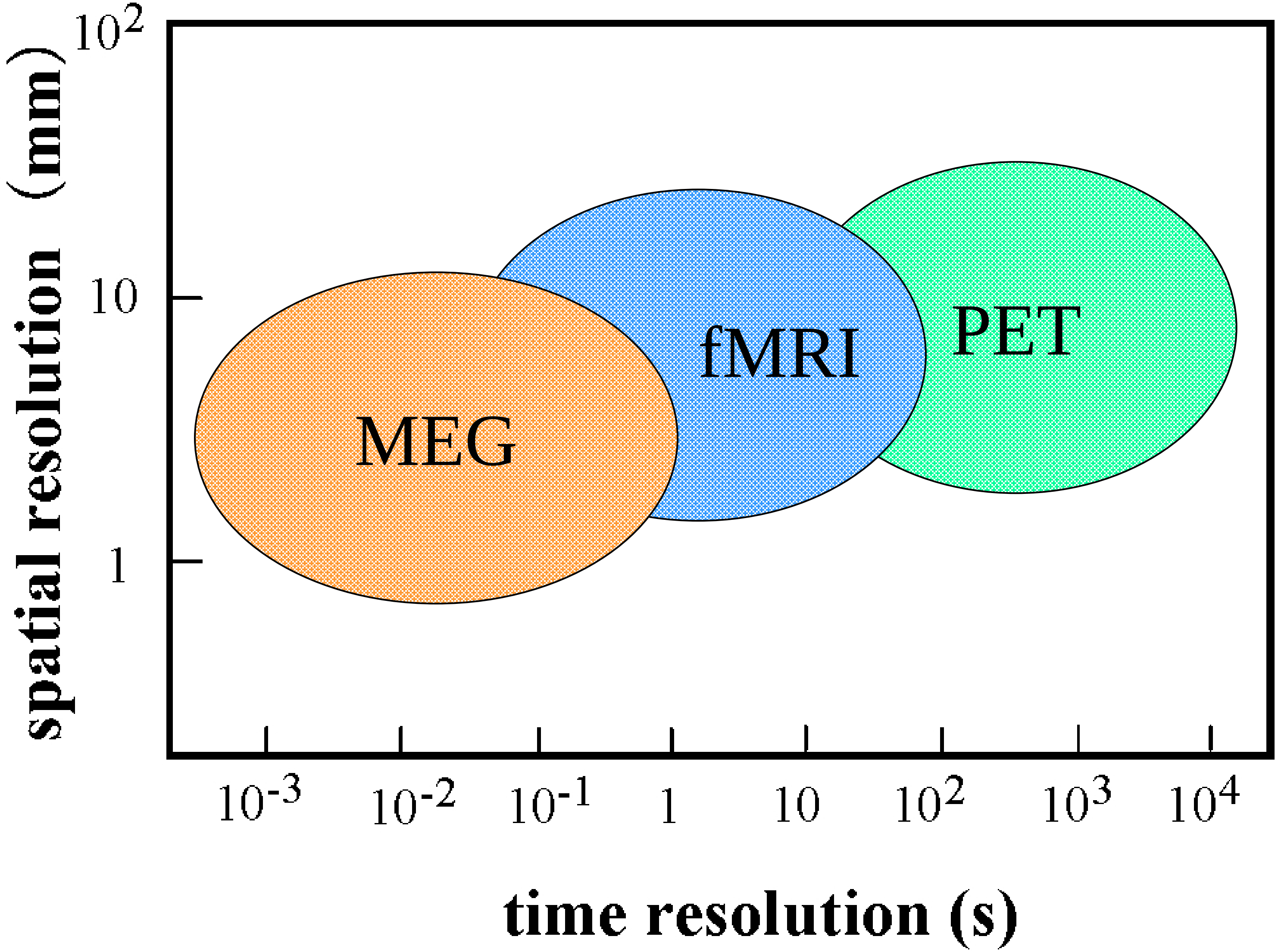

spatial resolution (mm)
10^2
10
1
MEG
fMRI
PET
10^{-3}
10^{-2}
10^{-1}
1
10
10^2
10^3
10^4
time resolution (s)

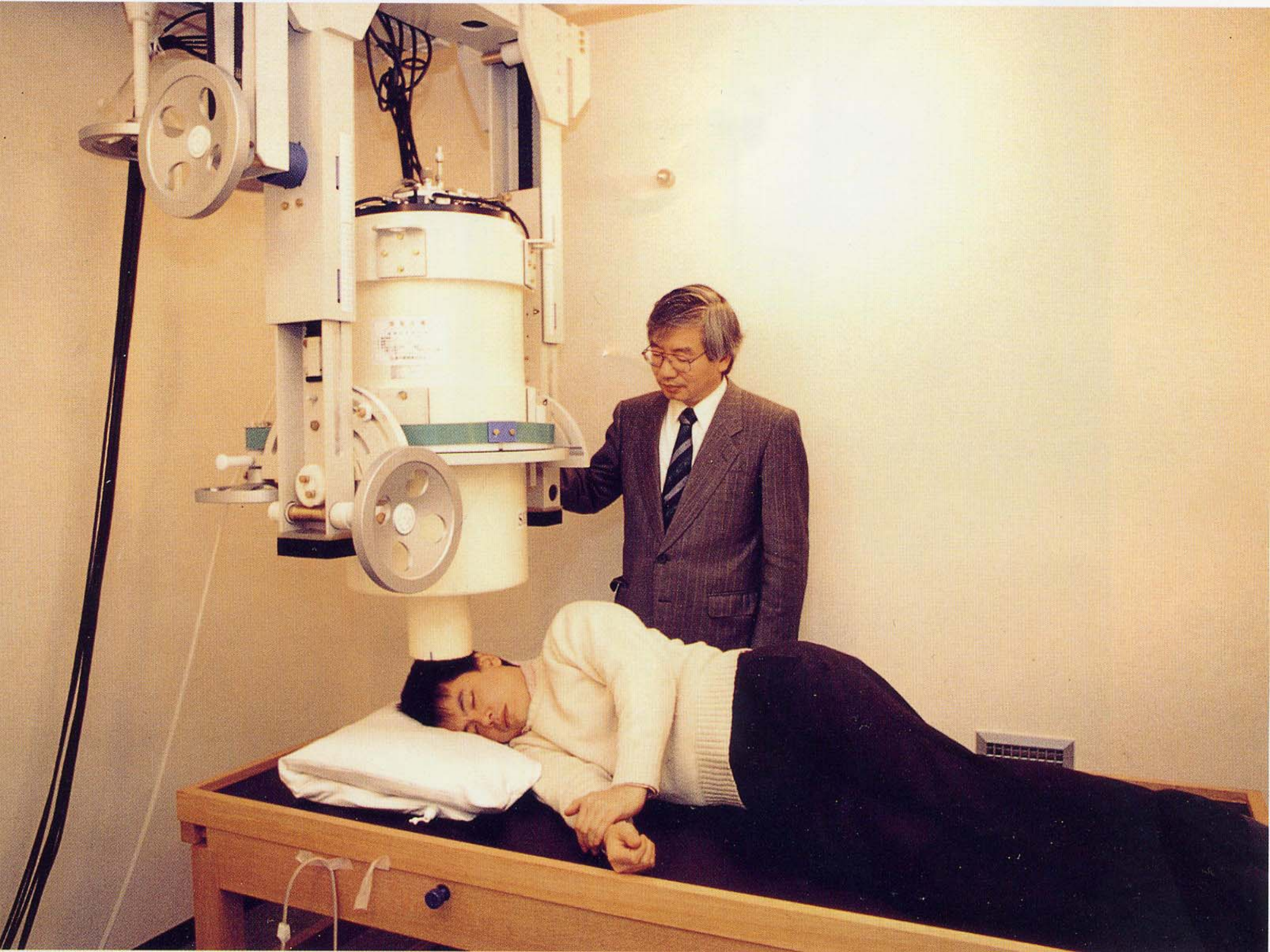

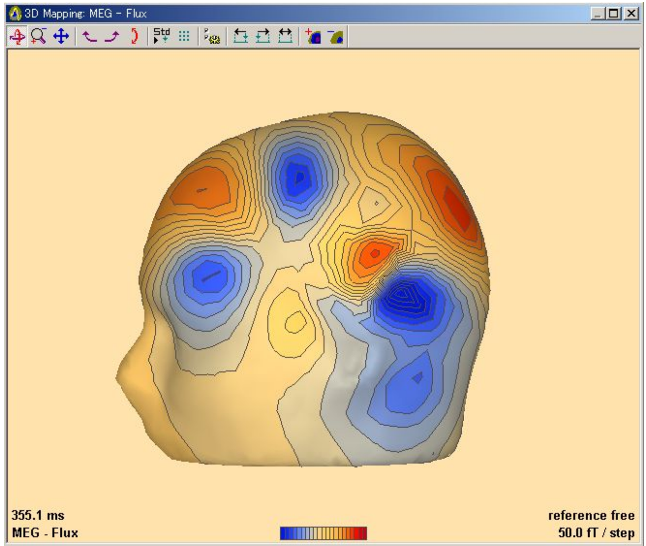
3D Mapping: MEG - Flux
355.1 ms
MEG - Flux
reference free
50.0 fT / step

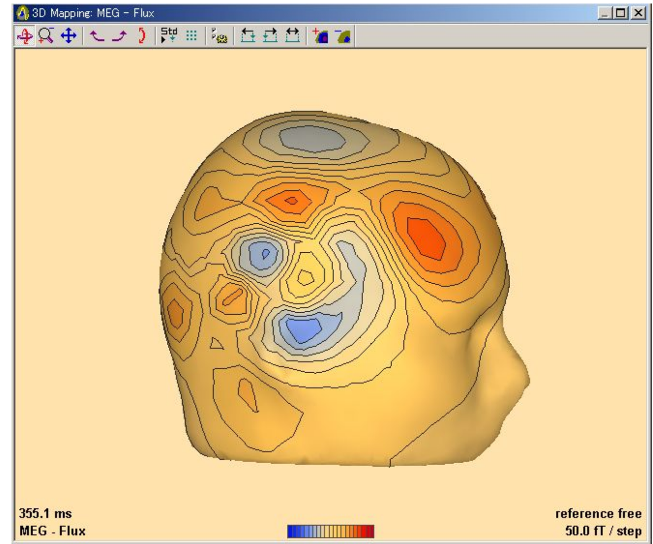
3D Mapping: MEG - Flux
355.1 ms
MEG - Flux
reference free
50.0 fT / step

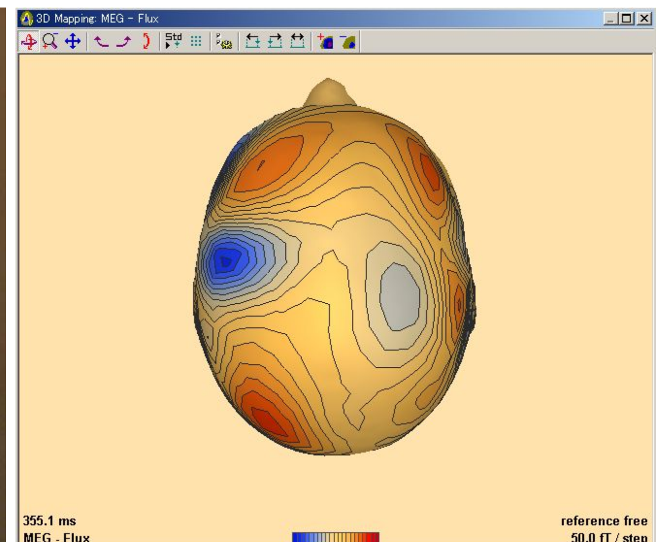
3D Mapping: MEG - Flux
355.1 ms
MEG - Flux
reference free
50.0 fT / step

Inverse Problem

I. Estimation of Current Dipoles

* Newton Iteration Method
* Marquardt's Method
* Simulated Annealing Method
* Genetic Algorithm

II. Estimation of Current Distribution

* Fourier's Transformation Method
* Pattern Matching Method
* Minimum Norm Estimation
* MUSIC (Multiple Signal Classification) Algorithm
* Sub-Optimal Least-Squares Subspace Scanning Method
* Spatial Filtering Method
* LORETA (Low Resolution Brain Electromagnetic Tomography)

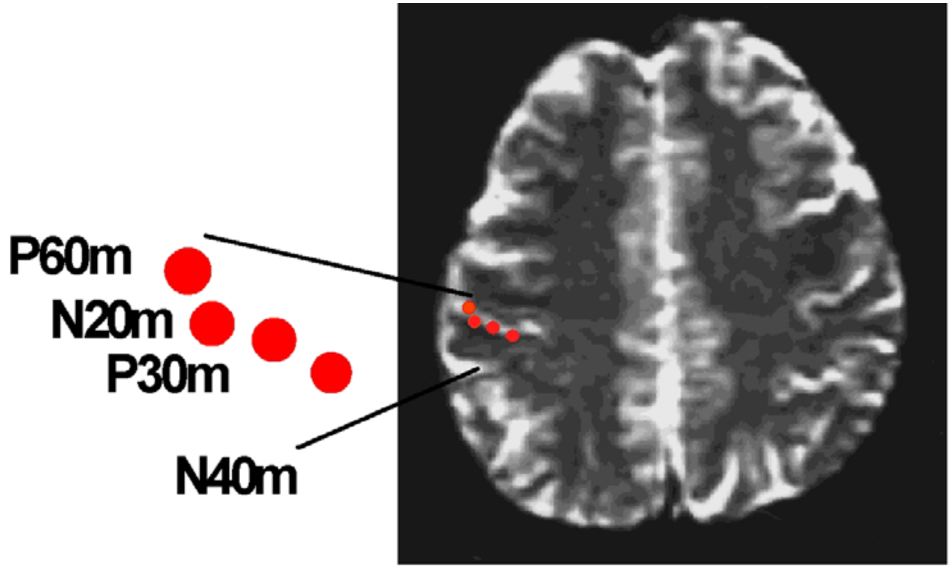

(a) MEG

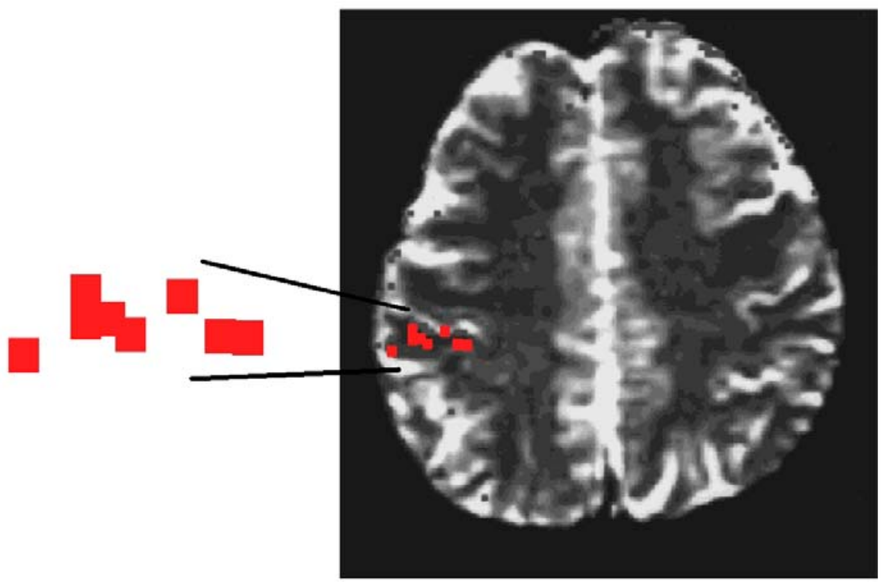

(b) fMRI

Mental rotation task

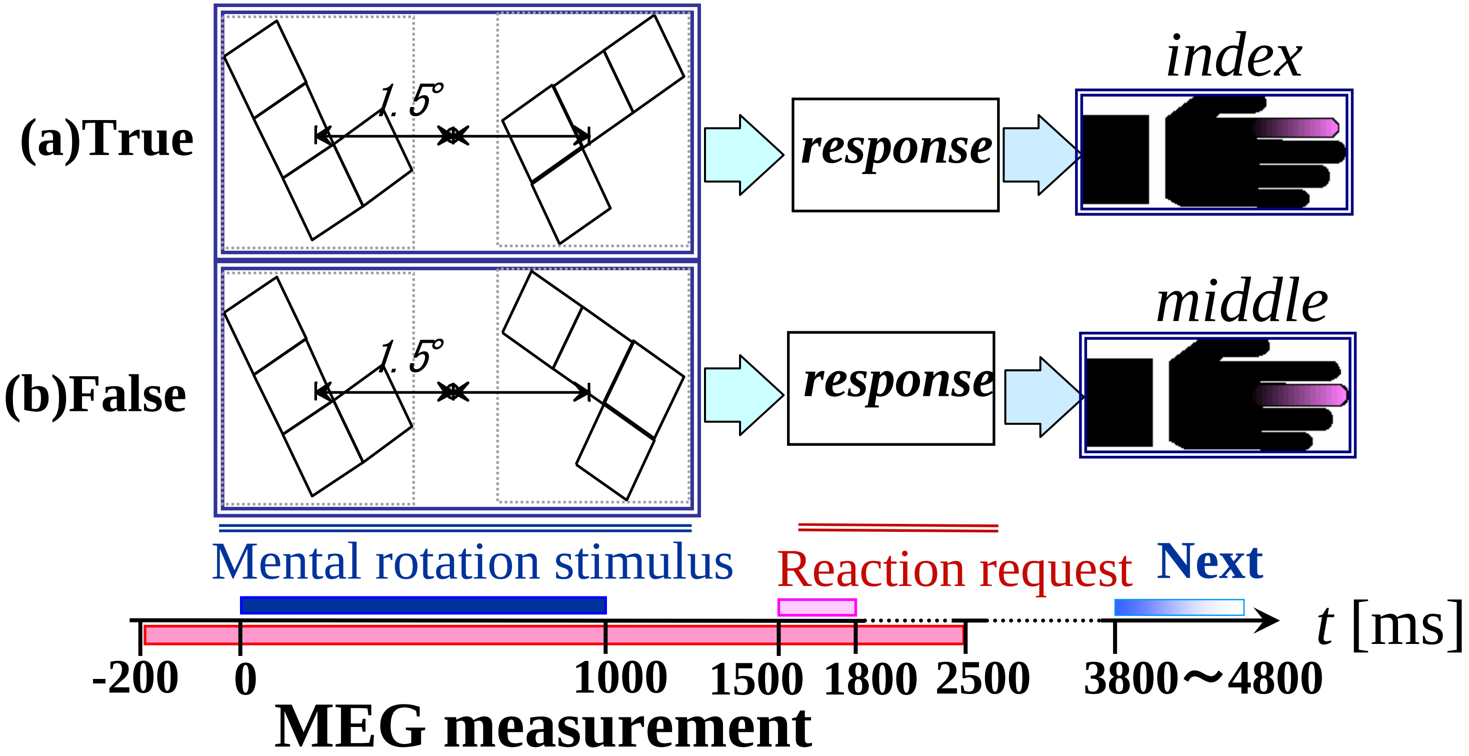

A mental rotation process requires rotation and matching of a pair of mental images.

Estimated source distributions (mental rotation)

Mental rotation task | **Control task**

180 ms

190 ms

210 ms

240 ms

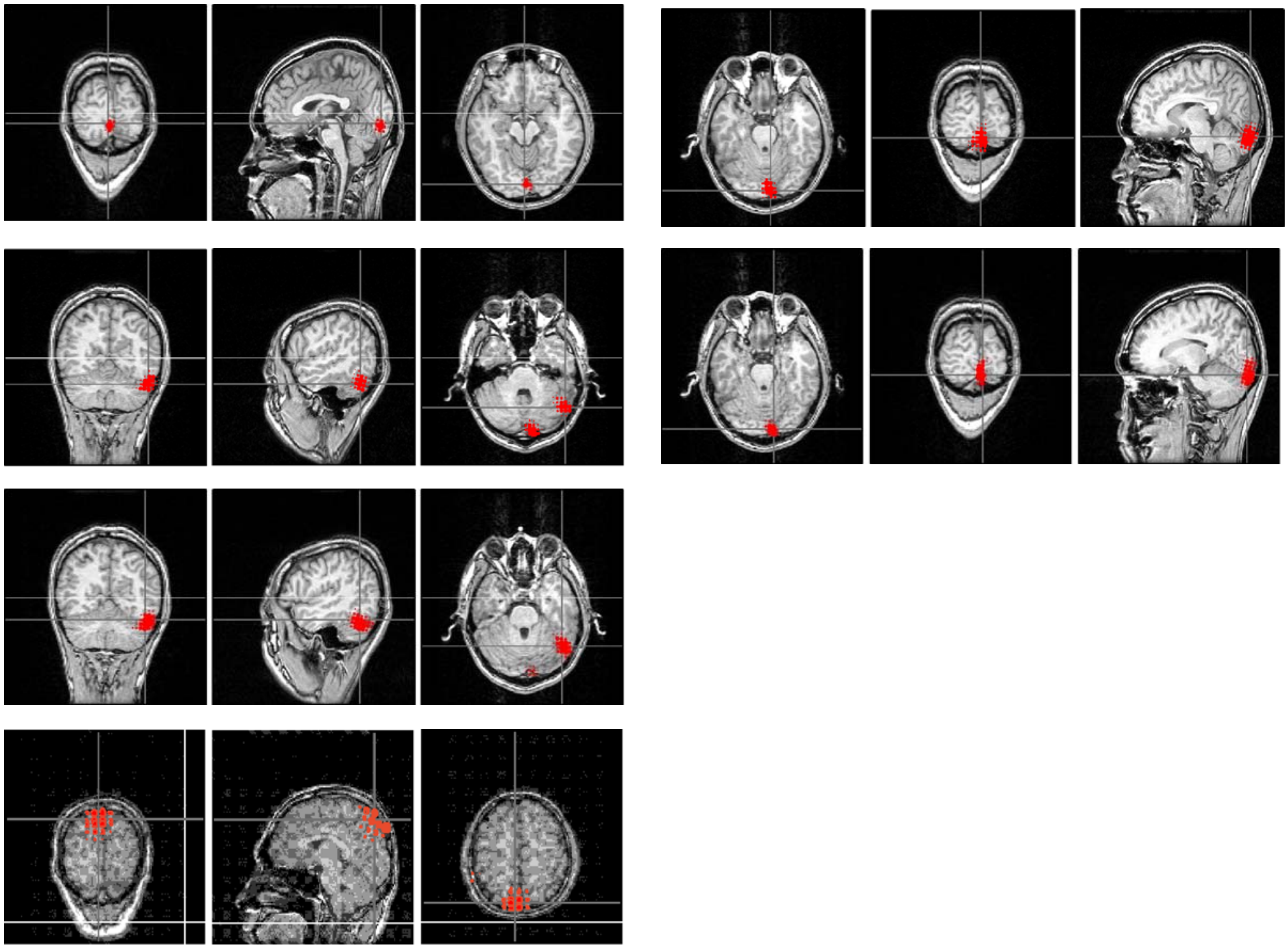

Functional MRI: Mapping of Language Areas by fMRI

Word generation – Speech for words starting with “A”

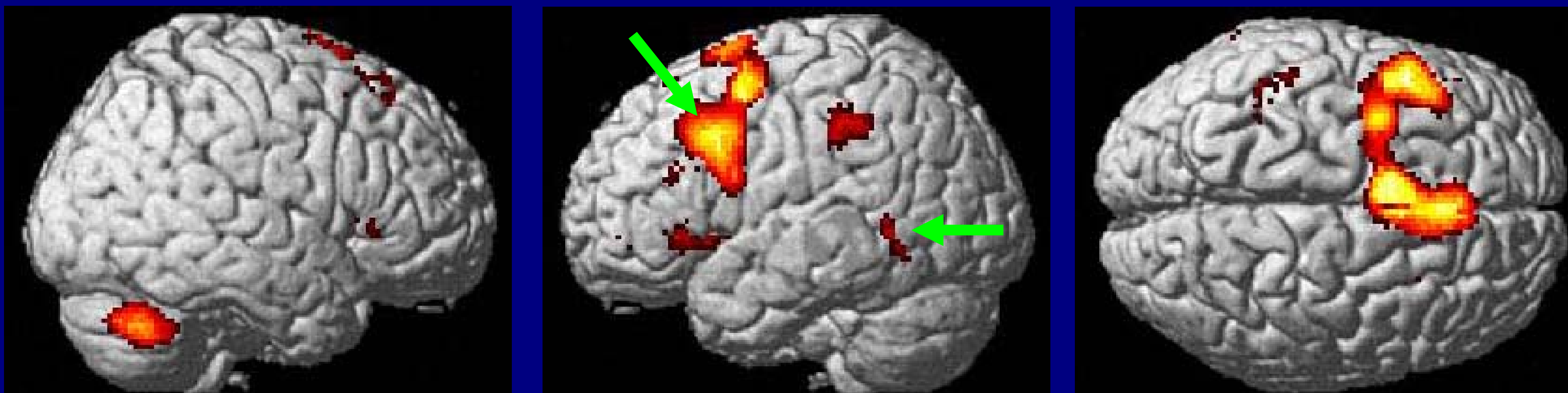

Verb generation – Conceptualization (door → open; chair → sit down)

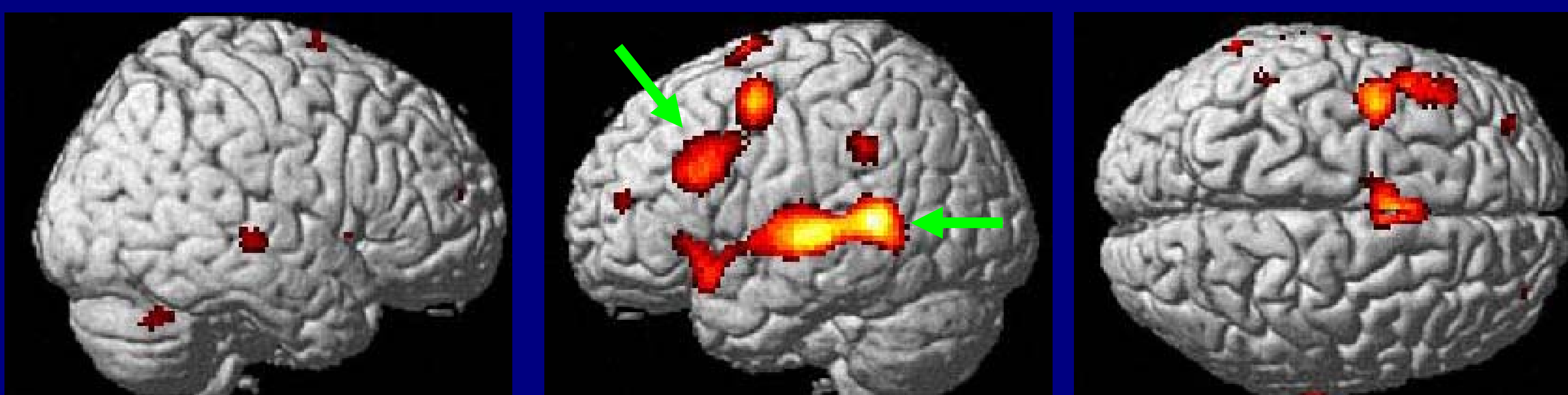

Courtesy of Dr. T. Yoshiura (Kyushu University)

Fibertractography of pyramidal tracts in a patient with a brain tumor

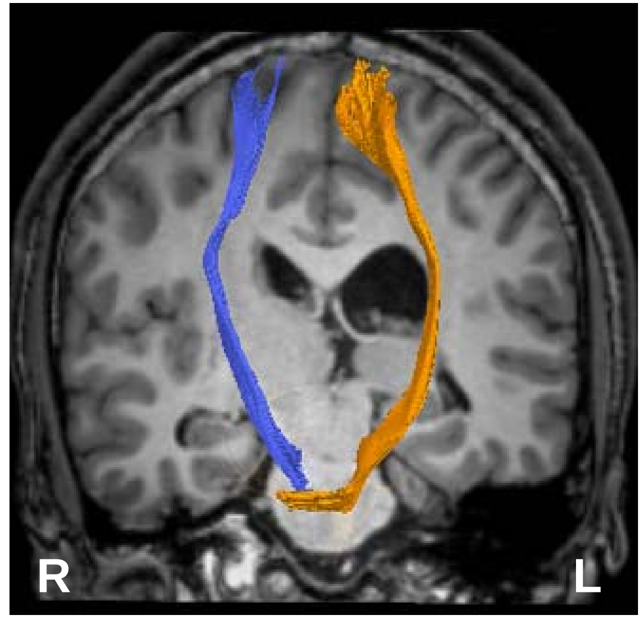

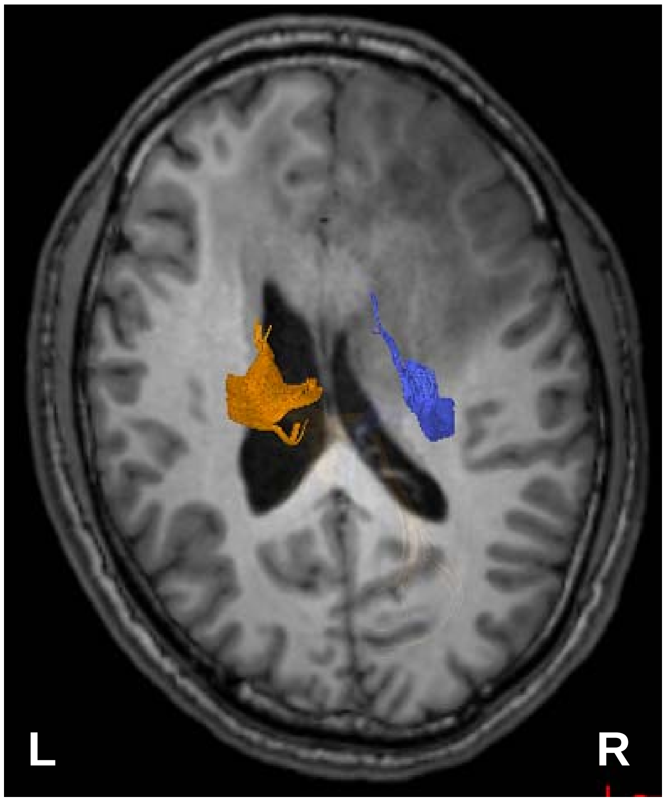

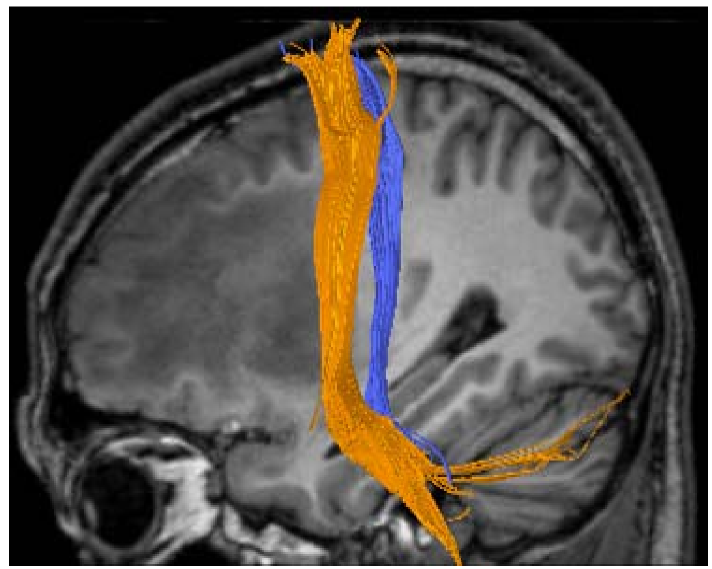

Courtesy of Dr. T. Yoshiura (Kyushu University)

Imaging of electrical information in the brain based on MRI

1. Impedance/Conductivity MRI

2. Electric Current MRI

Three different methods of impedance imaging based on MRI

1) A large flip angle method

2) Additional AC field method

3) A method based on diffusion tensor MRI

Impedance MRI based on a large flip angle method

- The principle of the impedance MRI by using large flip-angles is to use the variations in eddy current densities at the tissues induced by radio frequency (RF) waves at the resonant frequency that are generated by the RF coil in MRI.

- The MRI signals are disturbed by the eddy currents with a degree of disturbance that is dependent on the tissue inhomogeneities.

- Using RF currents with large flip angles we enhance this difference in the effect of the eddy currents on MRI signals at tissues with different impedance.

Series of image projections of phantom and mouse head using the large flip angle method

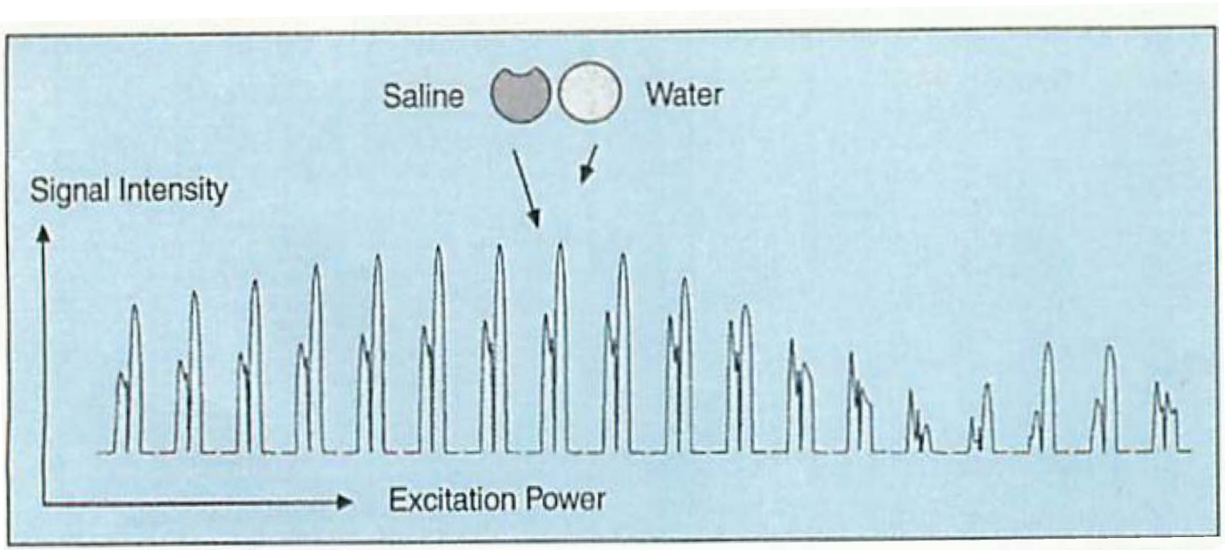

Series of image projections of water and saline solution phantom
obtained with excitation power increased stepwise from the left to the right.

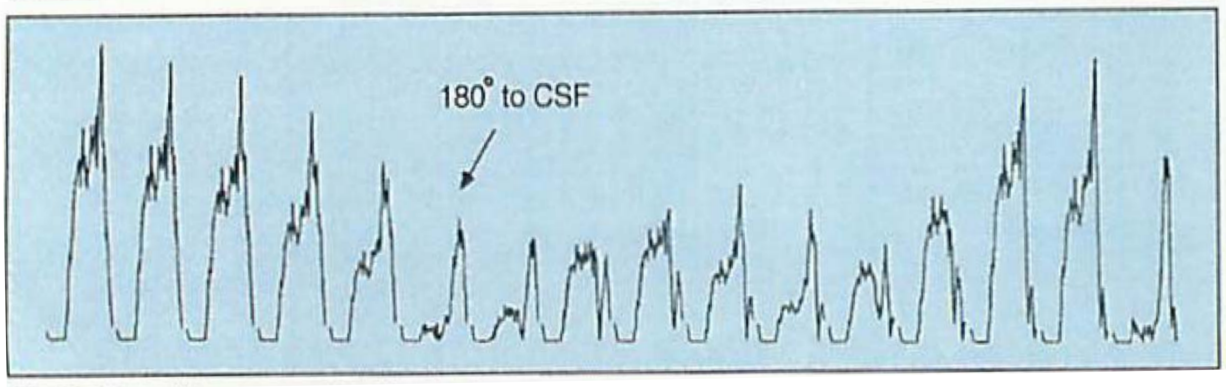

Series of image projections of the mouse head obtained with the excitation power increased stepwise from the left to the right.

Images of a rat's head at different spin-flip angles relative to the cerebrospinal fluid

160 °

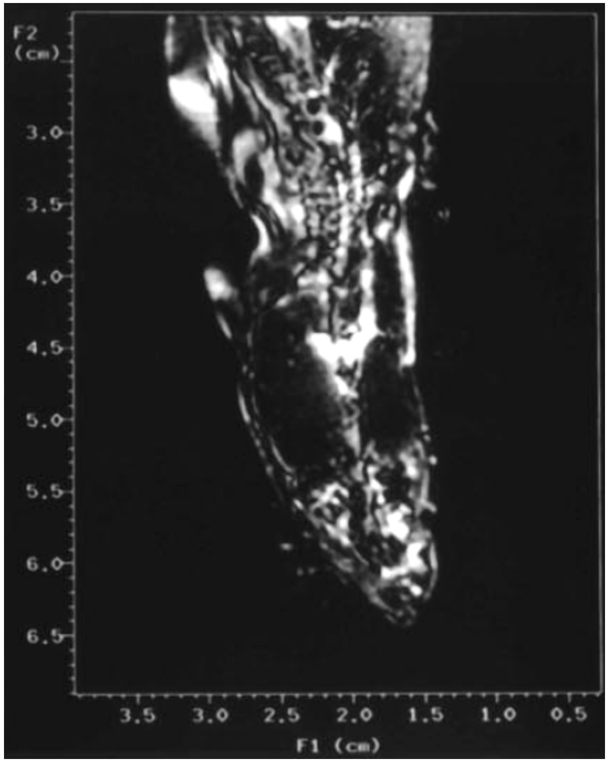

180 °

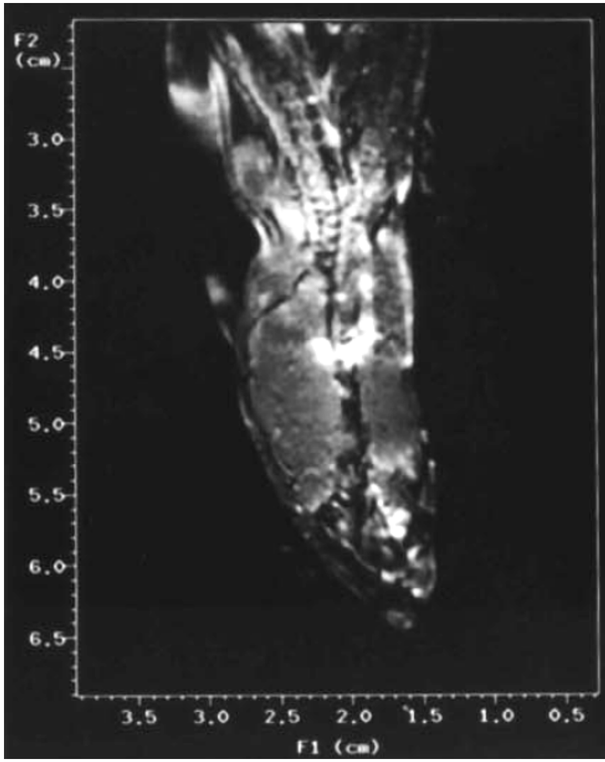

200 °

Impedance/Conductivity imaging based on diffusion tensor MRI

- The diffusion components of biological tissues are usually divided into a fast and a slow component.

↓

- Thanks to the proportionality between conductivity and diffusion coefficient, the tissue conductivity is estimated by measuring the first diffusion component, which corresponds to diffusion in the extracellular fluid.

↓

- The imaging contains the anisotropic information in the tissues.

Signal attenuation in the human brain

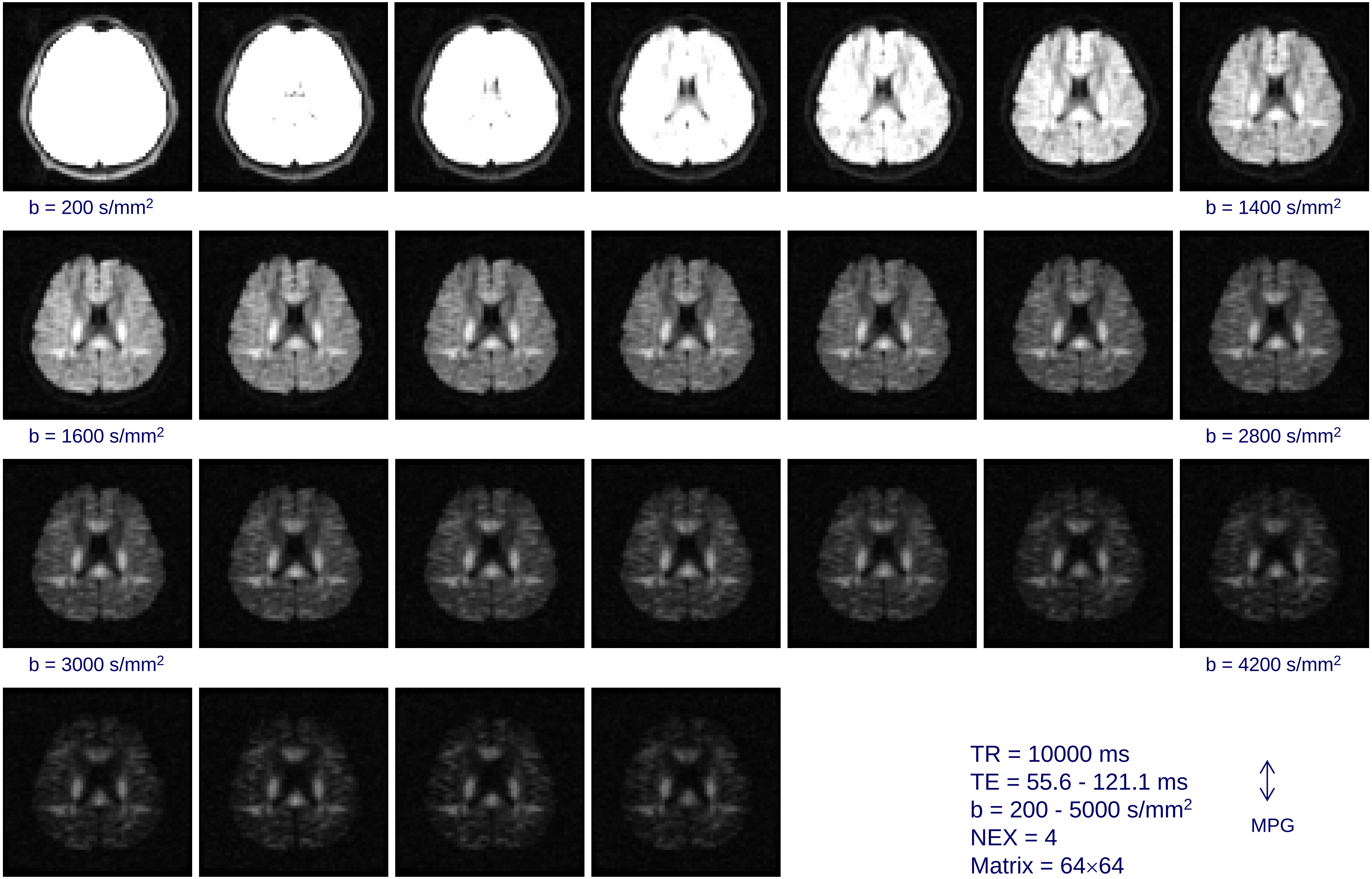

TR = 10000 ms
TE = 55.6 - 121.1 ms
b = 200 - 5000 s/mm^2
NEX = 4
Matrix = 64×64

↕
MPG

Conductivity images

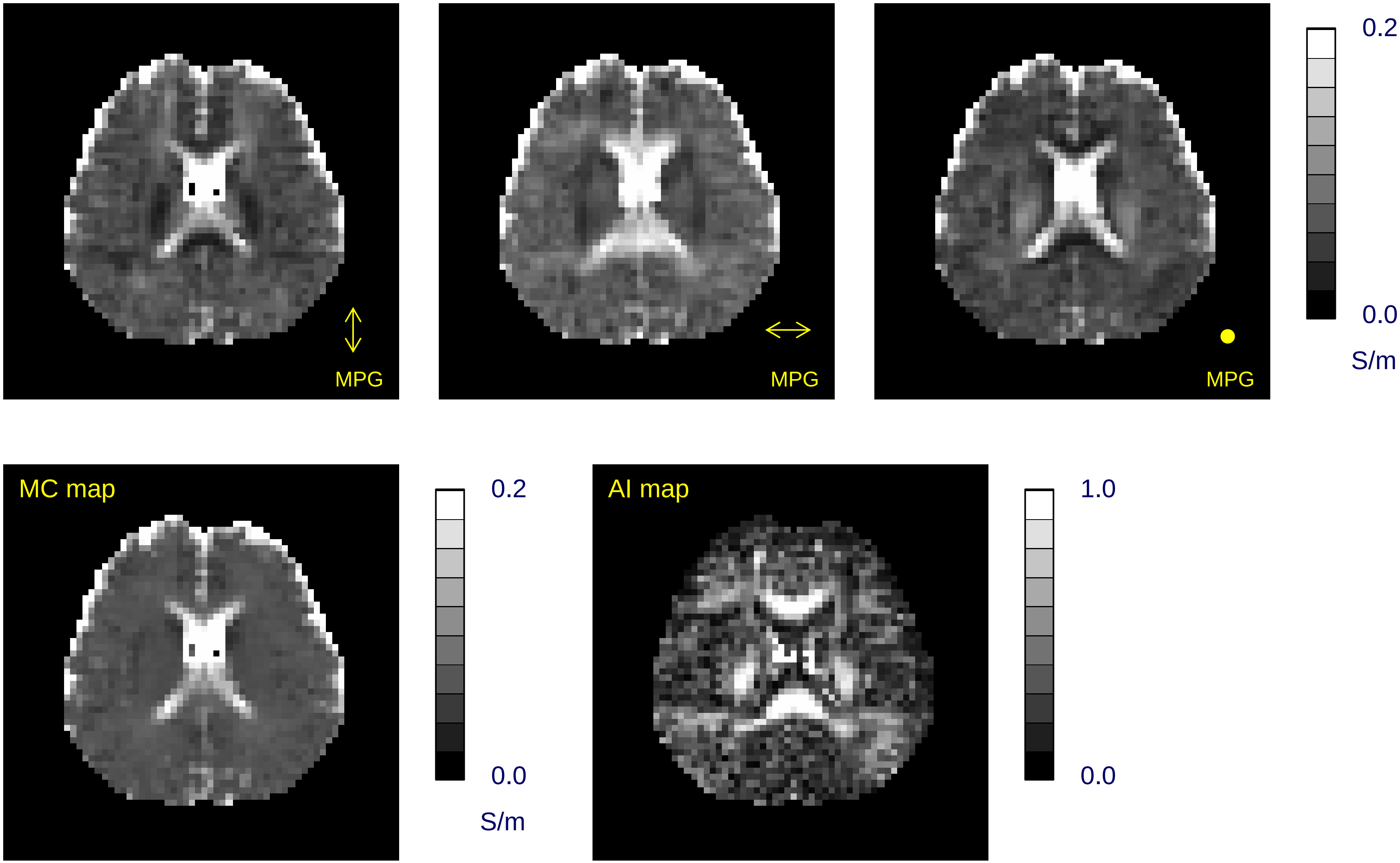

Electric current MRI

Method for non-invasively measuring current distributions in biological bodies using MRI

Potential applications:

1. Measurement of externally applied electric currents for the purpose of electric stimulation.
2. A new technique for functional imaging of the brain based on a detection of magnetic fields arising from neuronal electrical activities.

In this presentation, we introduce

1. Quantitative measurement of magnetic fields generated from an externally applied electric current.
2. Theoretical limit of sensitivity for detecting weak magnetic fields using MRI.
3. Detection of neuronal electrical currents in the rat brain

Phantom for experiments

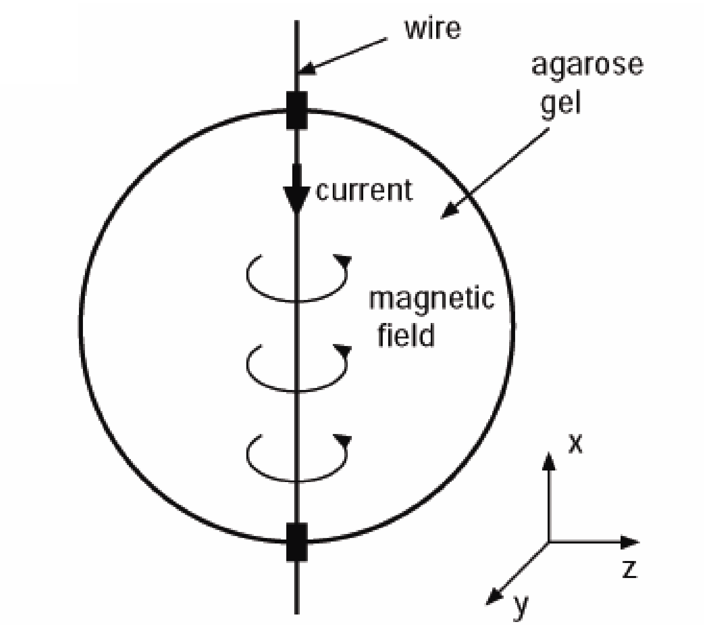

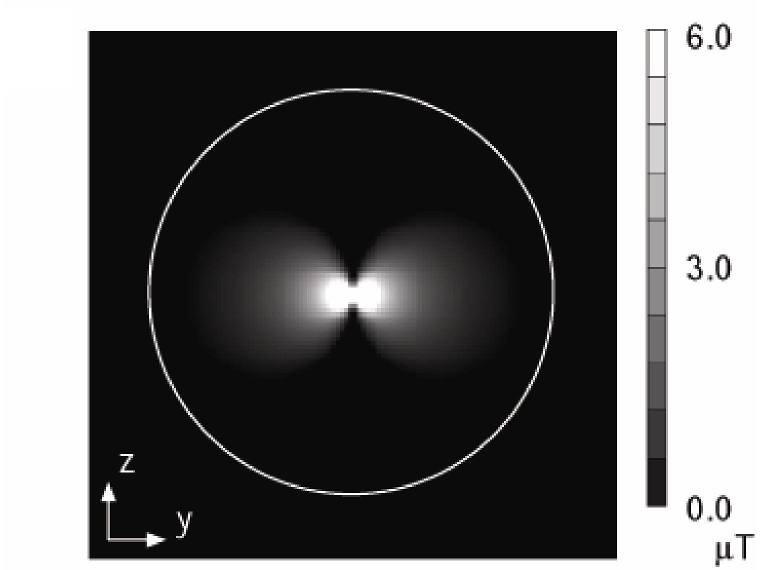

Diameter: 48 mm
1.0 % agarose / H_2O
Electric current: 100 mA

Theoretically calculated magnetic field component b_z.

$$b_z = \frac{\mu_0 I}{2\pi} \cdot \frac{\mathbf{r} \cdot \mathbf{e}_2}{|\mathbf{r}|^2}$$

Experimental Results

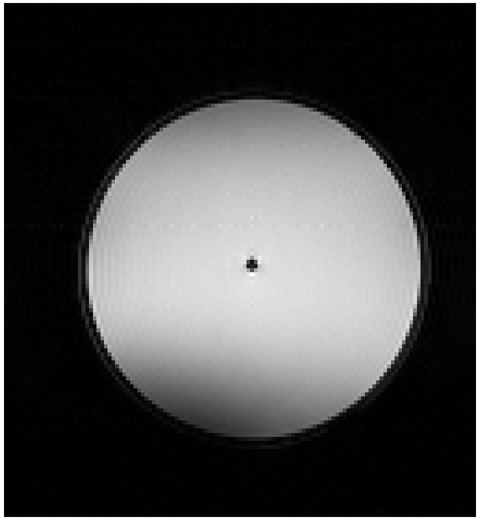

0 mA

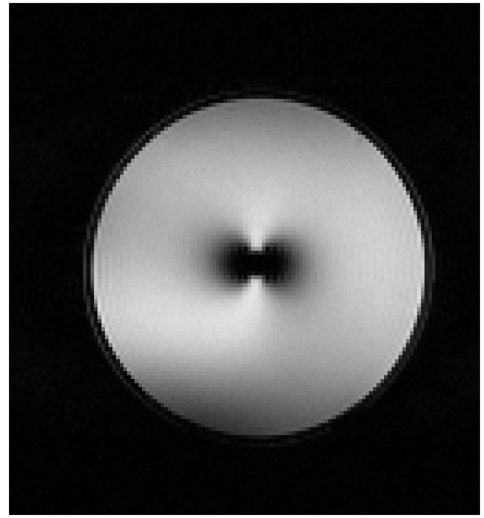

100 mA

T_R = 3000 ms
T_E = 60 ms
slice thickness = 4 mm
resolution = 500 μm

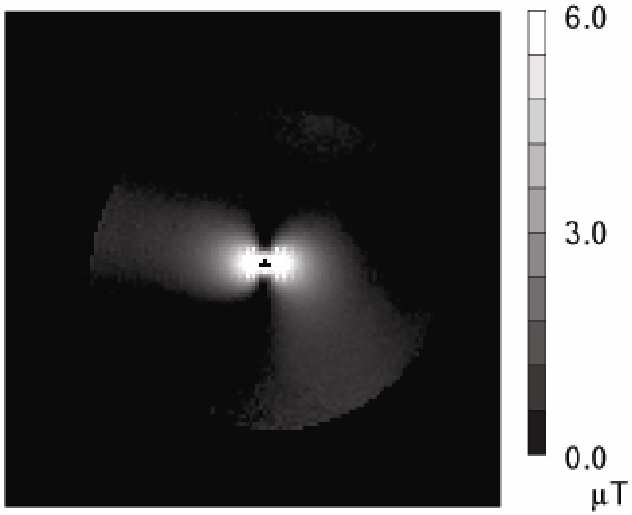

Experimentally determined magnetic field

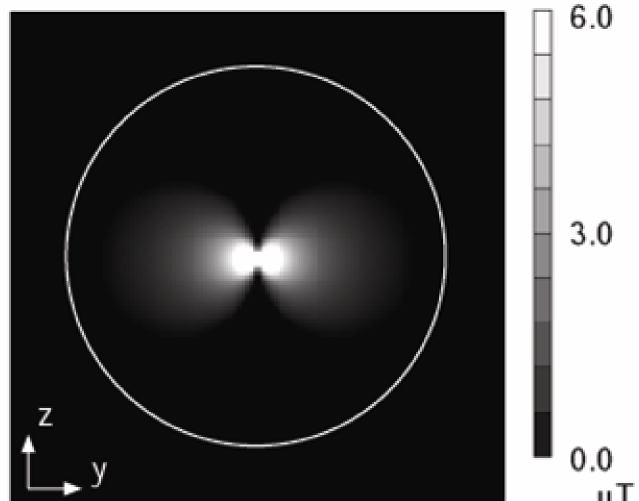

Theoretically calculated magnetic field

The experimentally determined magnetic field was in good agreement with the theoretically calculated magnetic field.

Discussion: Sensitivity for detecting weak magnetic fields using MRI

Magnetic fields attenuate with an increase in the distance from the neurons. Protons in close proximity to the neurons receive stronger magnetic fields in comparison with a detector located on the scalp.

Human: 5.0×10^{-12} T on the scalp (30 mm)

➡ 5.6×10^{-9} T at 1 mm from the neurons

Rat: 1.7×10^{-12} T on the scalp (5 mm)

➡ 4.3×10^{-11} T at 1 mm from the neurons

Theoretical limit of sensitivity with signal averaging

$$\sigma_B = \frac{N}{S\gamma T_E \sqrt{a}}$$

	Human	Rat
Repetition time (T_R)	400 ms	333 ms
Echo time (T_E)	5 ms	30 ms
Static field (B_0)	1.5 T	4.7 T
RF field (B_1)	2×10^{-6} T	3.5×10^{-5} T
Field of view (L)	220 mm	32 mm
Slice thickness (h)	6 mm	2 mm
Flip angle (θ)	90°	20°
Number of pixels (n)	256	64
Resistance (R)	1.17 Ω	0.08 Ω
Number of averages (a)	100	100
Limit of sensitivity (σ_B)	2.6×10^{-9} T	1.9×10^{-11} T

The limit of sensitivity was below the intensity of magnetic fields in close proximity to the neurons for both the human and the rat. These results suggest that MRI has an enough sensitivity to the magnetic fields generated from neurons.

Time course of the signal intensity in the somatosensory cortex

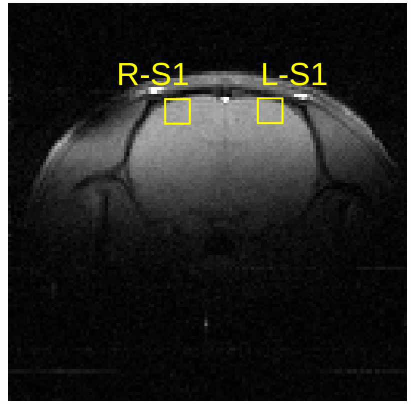

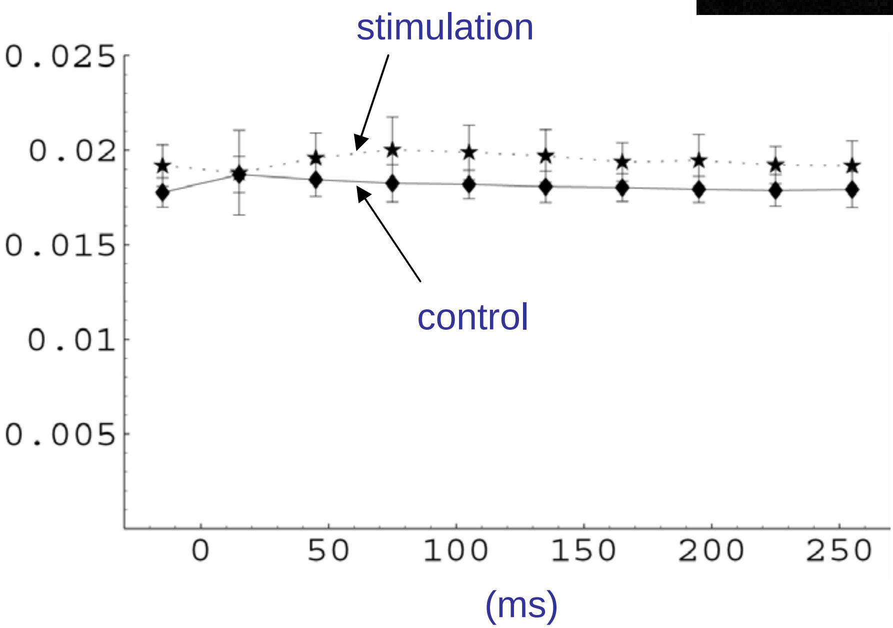

right somatosensory cortex

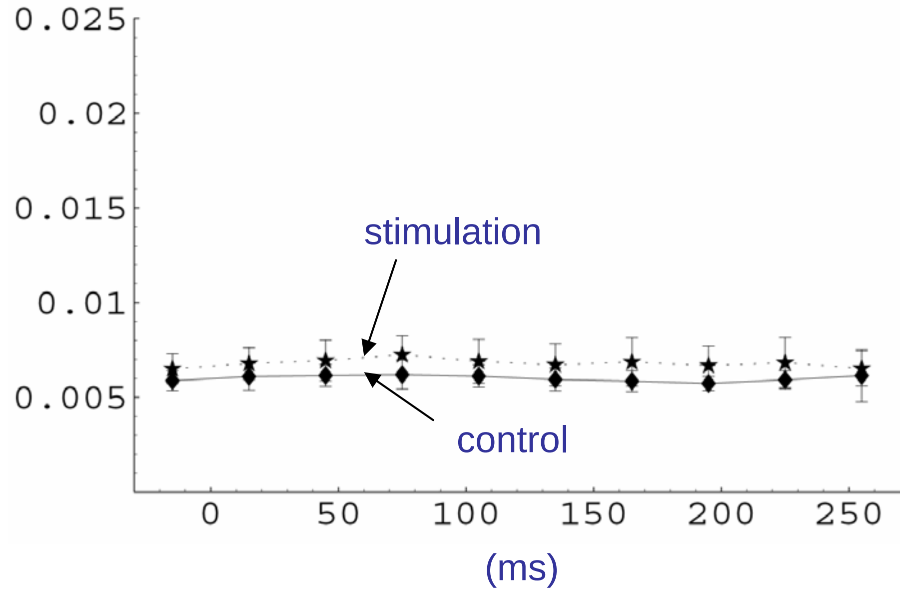

left somatosensory cortex

Comparison of the signal intensity between the images obtained at adjacent time points after electric stimulation

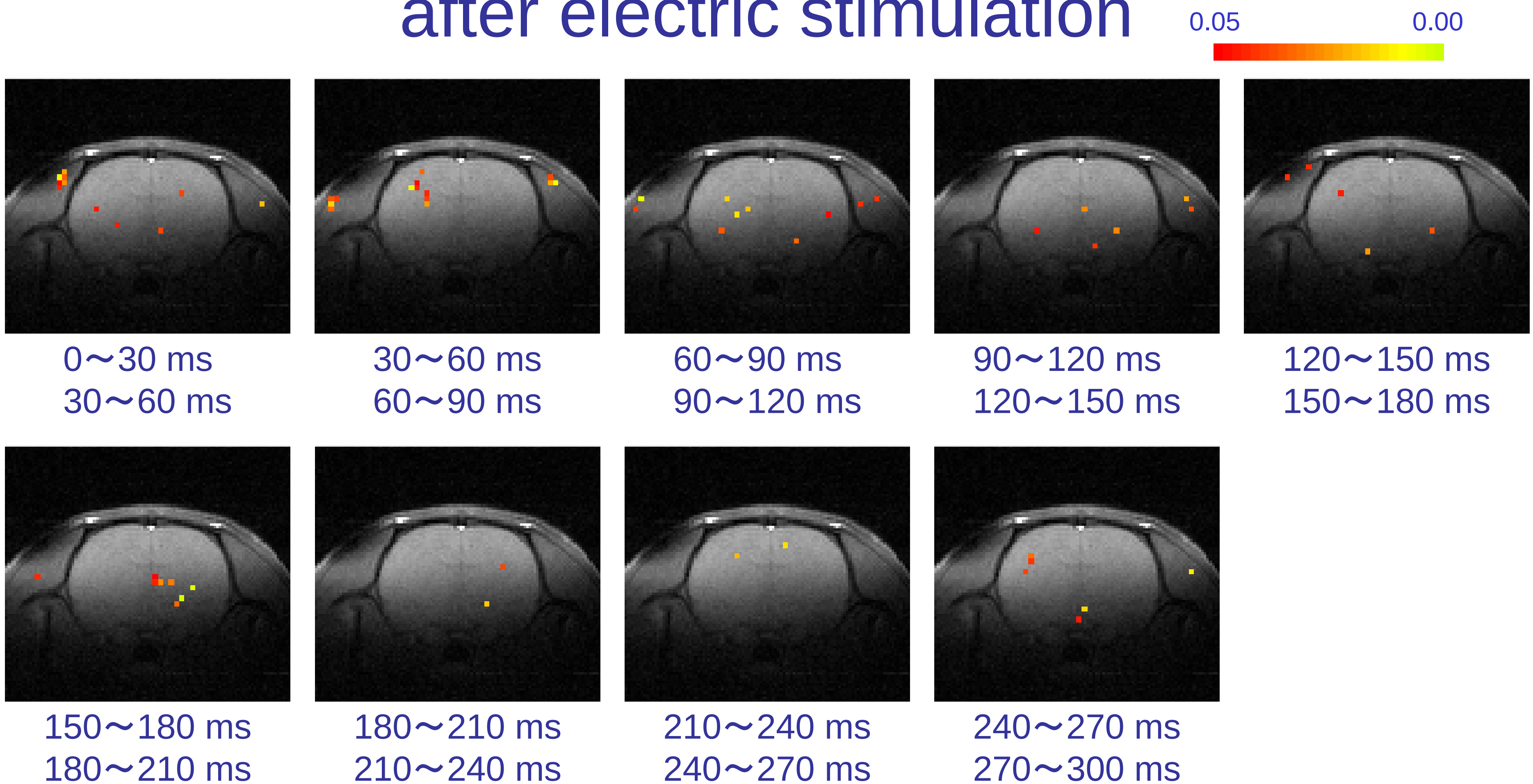

In the comparison between the 60-90 ms image and the 90-120 ms image, a temporal difference in the signal intensity was observed in the right somatosensory cortex. This reflects a decrease in the signal due to the weak magnetic field.

Destruction of Targeted Cancer Cells Using Magnetizable Beads and Pulsed Magnetic Force

Cells: TCC-S (Leukemic cells) expressing
CD33 antigen

Beads: Dynabeads Pan Mouse IgG (Dynal),
diameter = 4.5 ± 0.2 µm,
magnetic mass susceptibility
$= (16 \pm 3) \times 10^{-5}\ m^3/kg$

Dynabeads:

mono-sized, superparamagnetic, macroporous particles with narrow pores, in which magnetizable materials are distributed in the pores throughout the whole volume of the particles.

TCC-S cells and beads were bound together by an antigen-antibody reaction →cell/bead/antibody complex

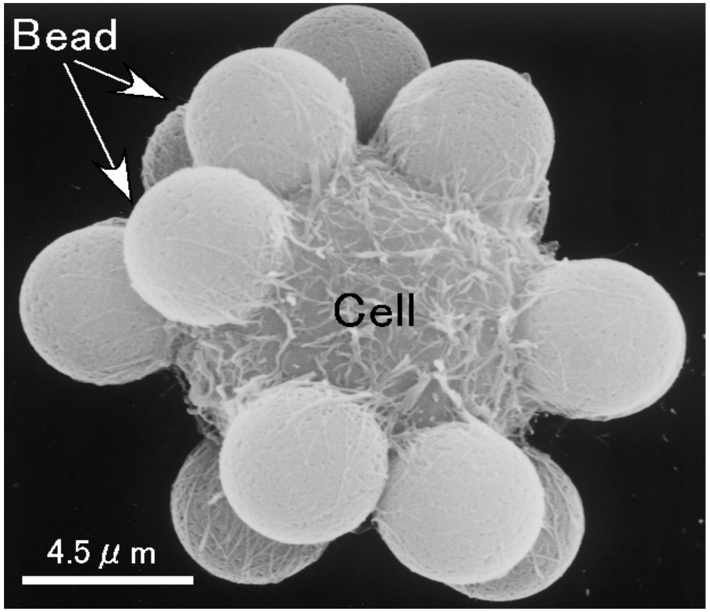

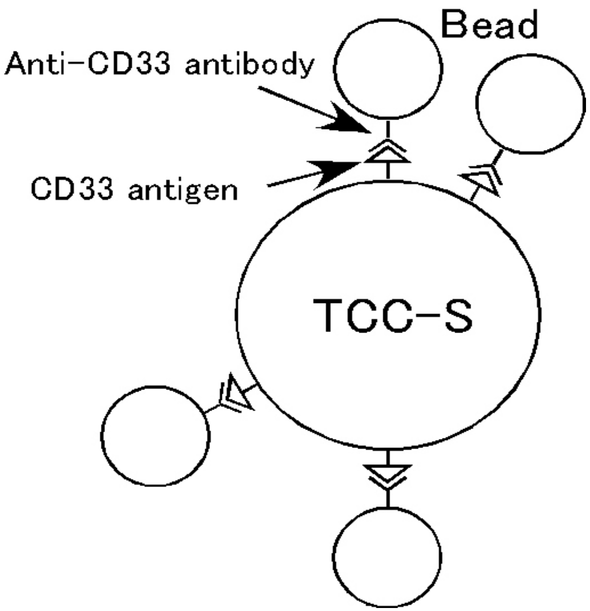

Electron scanning micrograph of the stimulates and nonstimulated cell/bead/antibody complex

Nonstimulated

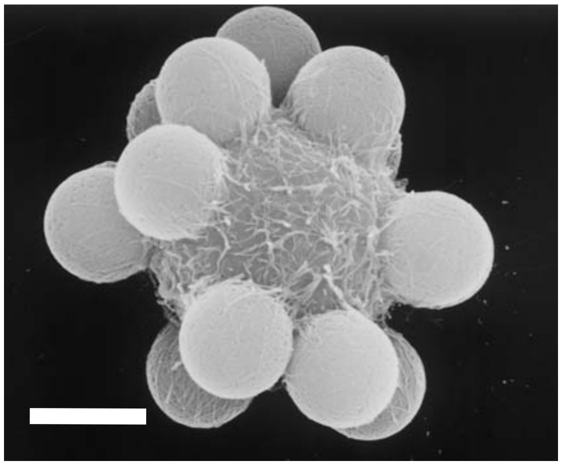

Stimulated

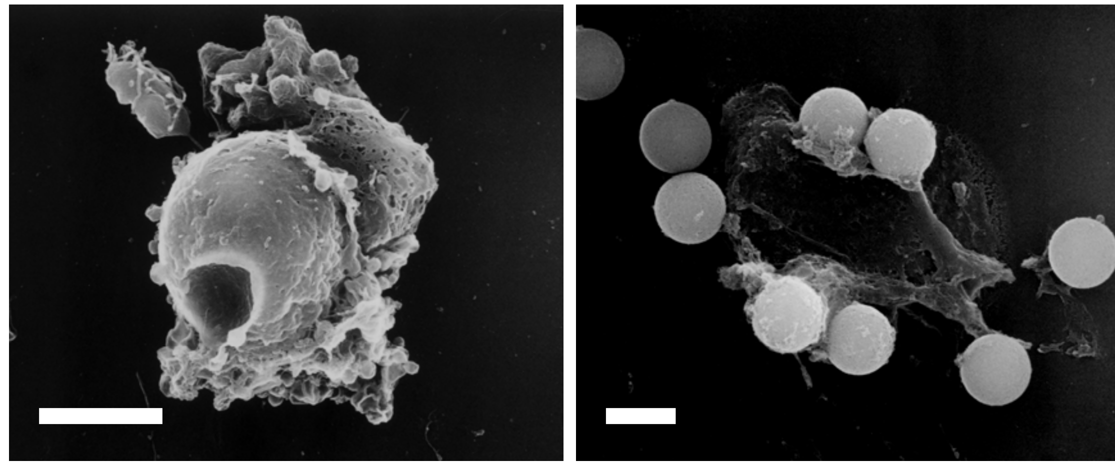

Scale bars = 4.5 μm

The cells were damaged by penetration of the beads or rupturing by the beads.
The instantaneous pulsed magnetic forces cause the beads to forcefully penetrate or rupture the targeted cells.

Mechanisms of biological effects of electromagnetic fields

1) Time-varying magnetic field

eddy currents $J = -\sigma \dfrac{\partial B}{\partial t}$

nerve stimulation

heat $SAR = \sigma \dfrac{E^2}{\rho}$

thermal effects

2) Static magnetic fields

i) homogenous magnetic field

magnetic torque

$$T = -\frac{1}{2\mu_0} B^2 \Delta\chi \sin 2\theta$$

magnetic orientation of biological cells

ii) inhomogeneous magnetic field

magnetic force

$$F = \frac{\chi}{\mu_0} (\mathrm{grad}\ B)\ B$$

parting of water by magnetic fields (Moses effect)

3) Multiplication of magnetic fields and other energy

photochemical reactions with radical pairs

singlet-triplet intersystem crossing

yield effect of cage -product and escape -product


STRONG
MAGNETIC FIELDS

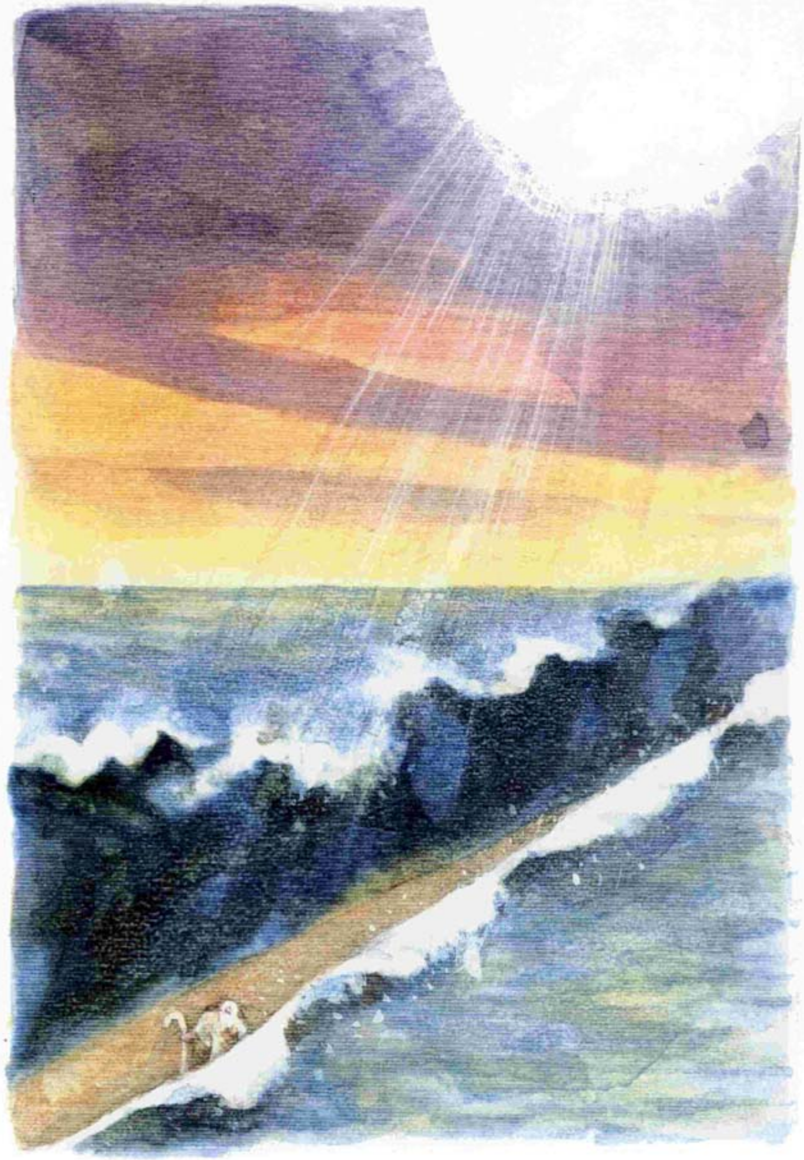

モーゼ　紅海を分ける　　　Moses parted the Red Sea

Magnetic orientation of adherent cells

Direction of magnetic field

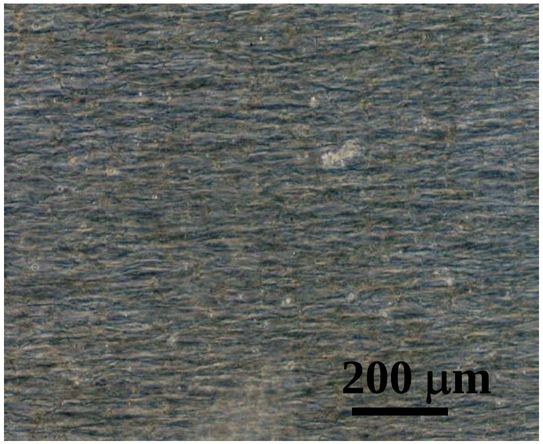

fibrin

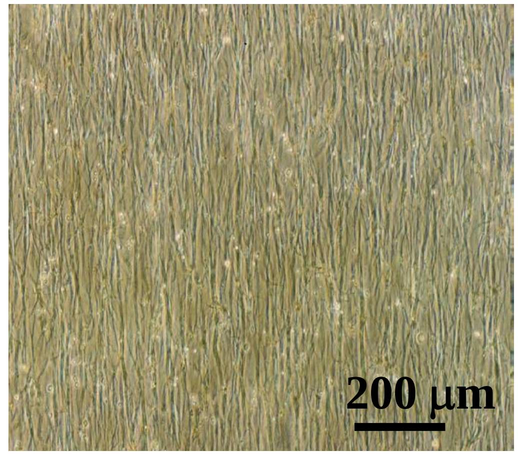

collagen

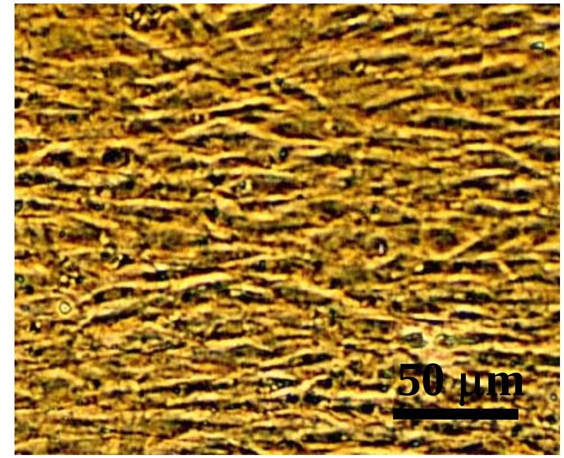

osteoblasts

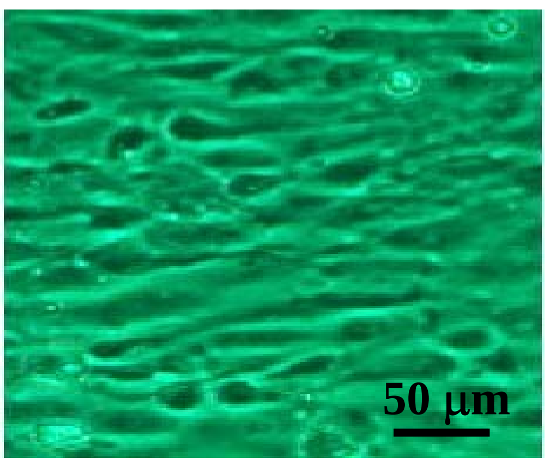

endothelial cells

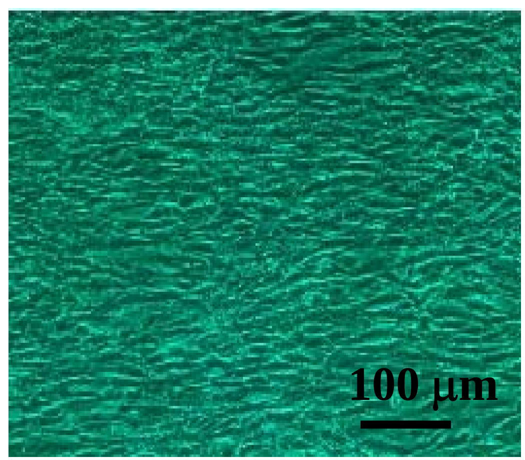

smooth muscle cells

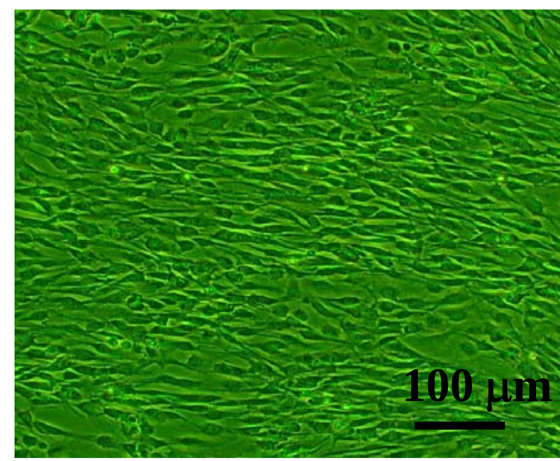

Schwann cells

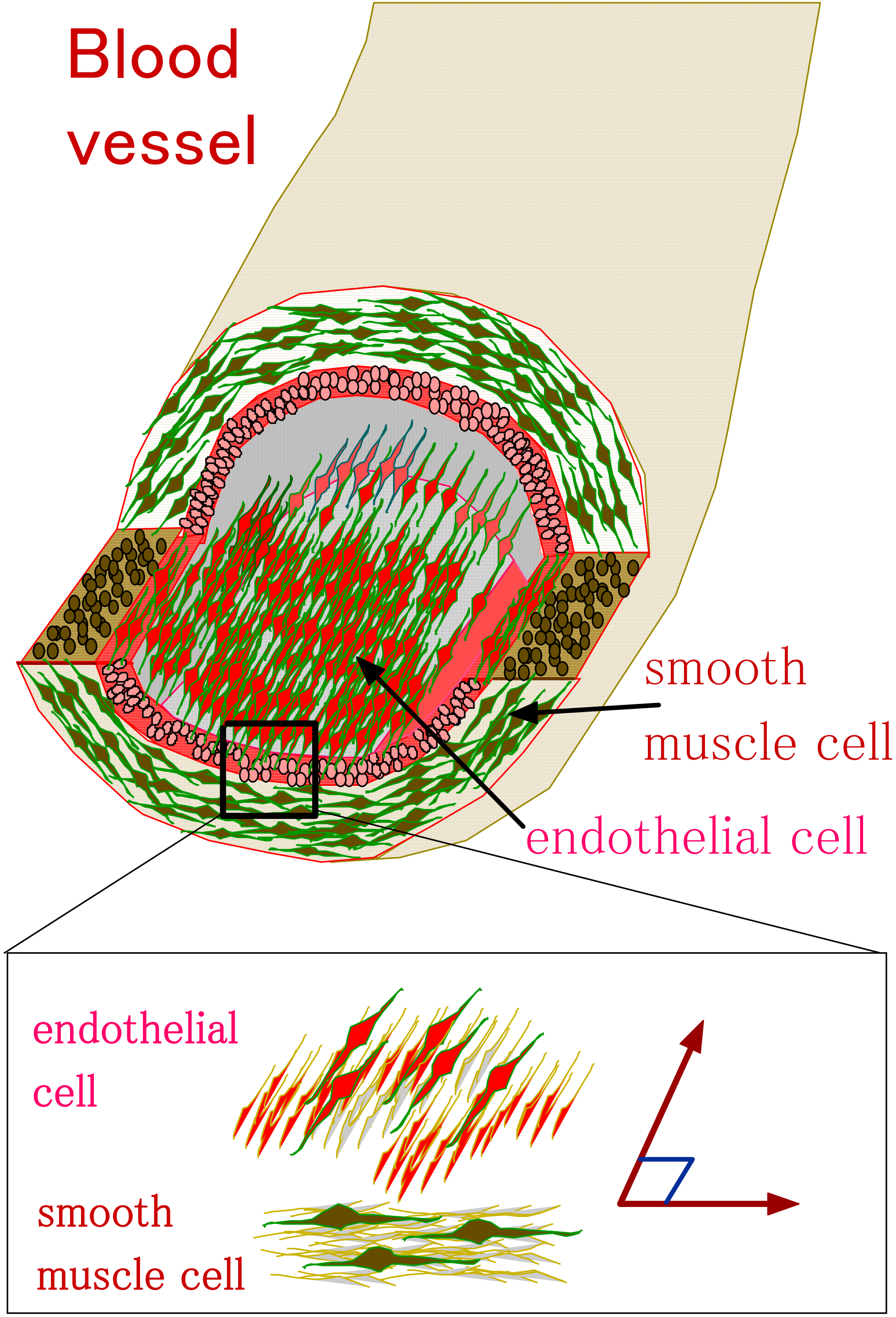
Blood vessel
smooth muscle cell
endothelial cell
endothelial cell
smooth muscle cell

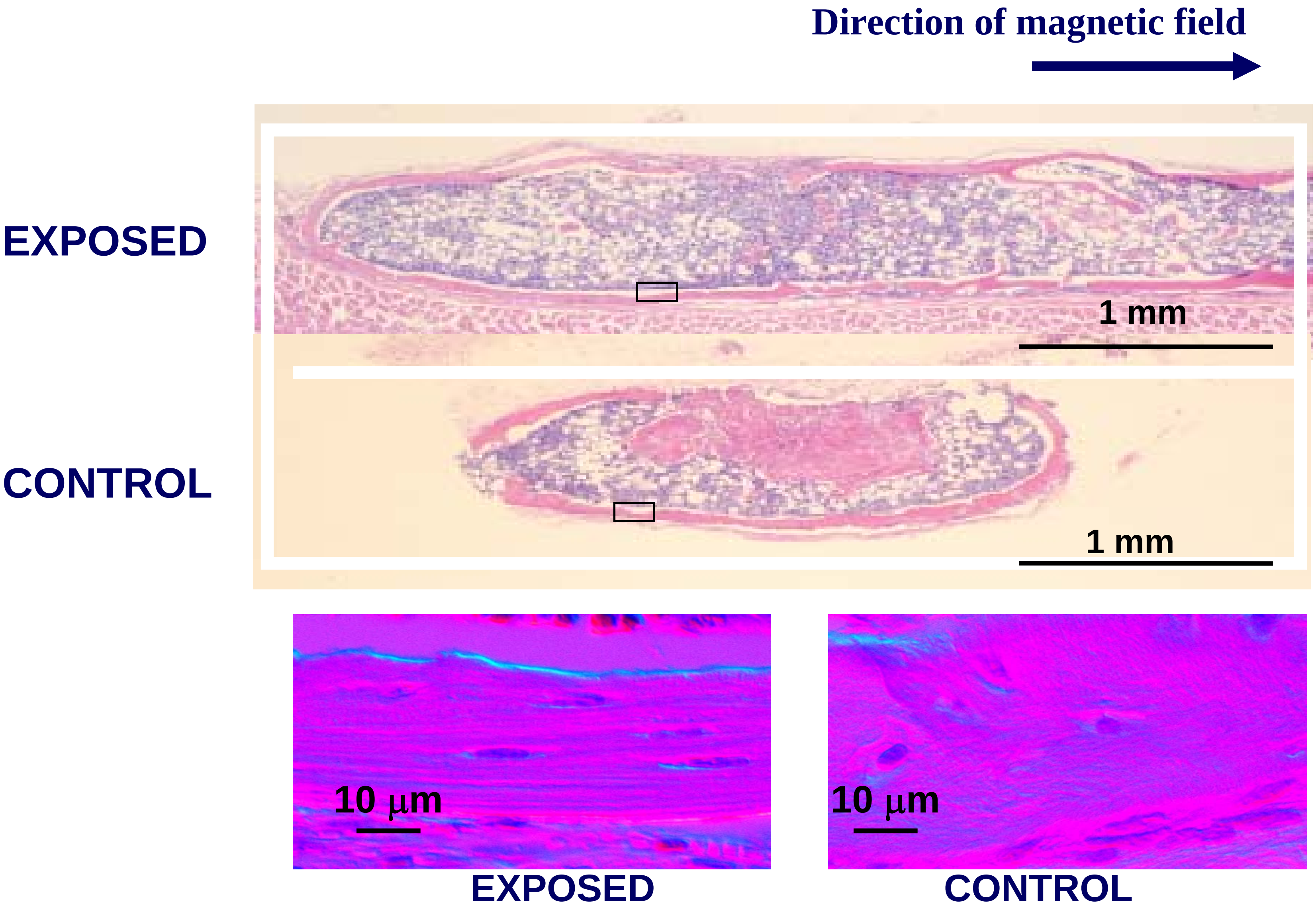

Ectopic bone formation was stimulated in and around subcutaneously implanted BMP-2 (bone morphogenetic protein)/collagen pellets in mice 21 days after 8 T magnetic field exposure for 60 h. The newly formed bone was extended parallel to the direction of the magnetic field.

Wallerian degeneration & sprouting

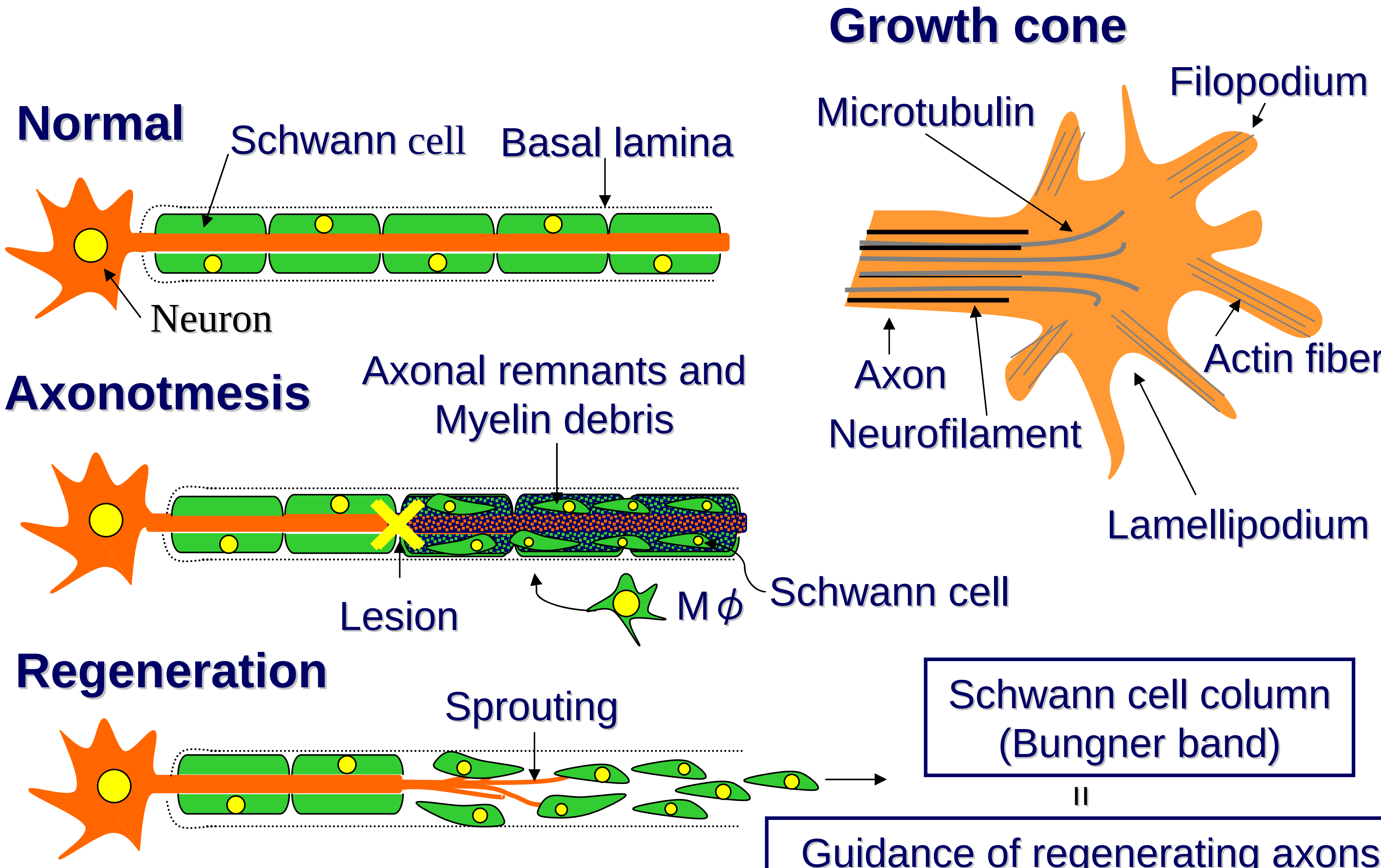

Schwann cell column (Bungner band)

II

Guidance of regenerating axons

Axon elongation into magnetically aligned collagen

Mixture of PC12 (rat pheochromocytoma) cells and collagen (5 days)

Control

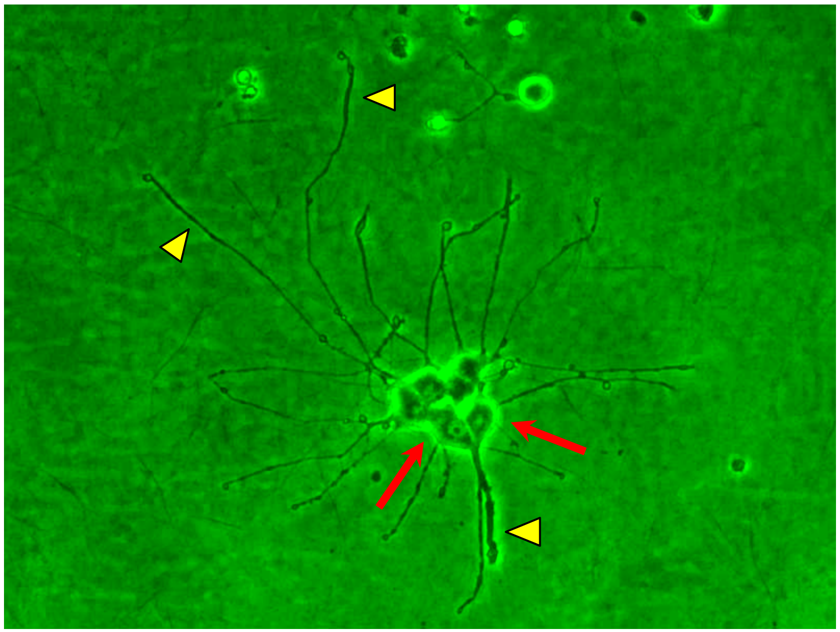

← : soma
◁ : axon

50 μm

Exposed

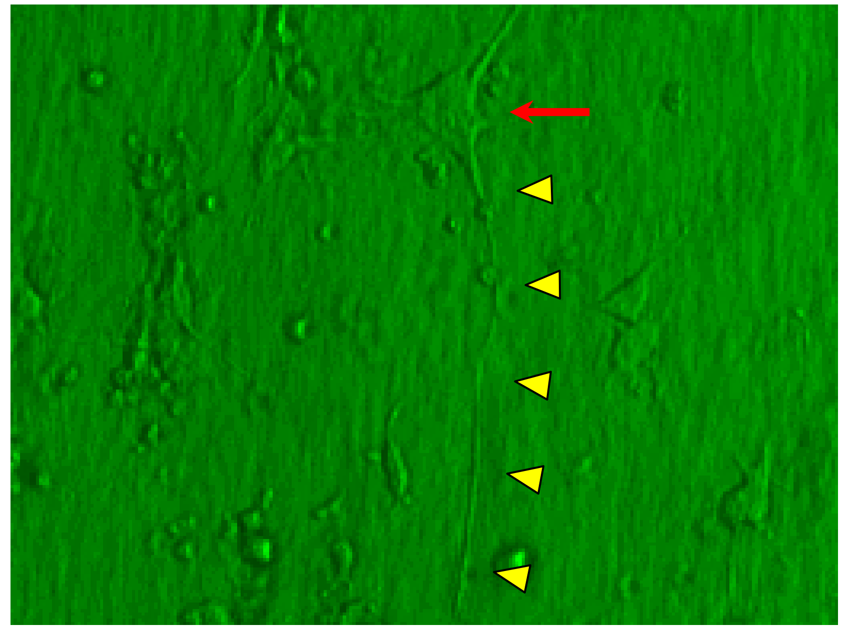

← : soma
◁ : axon

magnetic field →

50 μm

Orientation of collagen fibers ↑

Magnetically aligned collagen provides a scaffold for neurons on which to grow and direct the growing axon.

Morphological examination（12 W)

Control

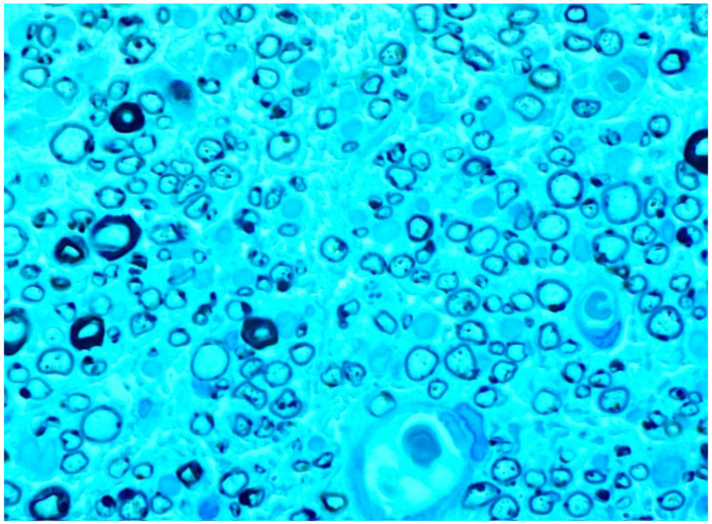

Exposed

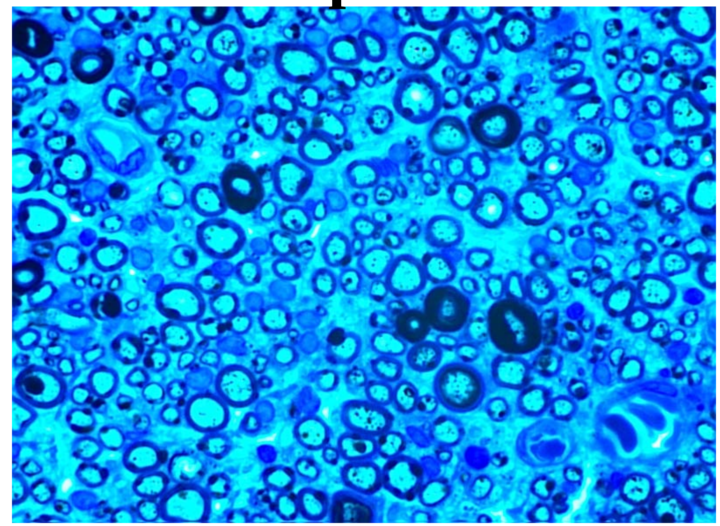

Numbers and diameters of myelinated fibers (po.12W)

	Control	**Exposed**
Numbers	274.0±11.7	373.4±27.6**
Diameters (μm)	5.53±0.064	5.81±0.087*

*p<0.05, **p<0.01

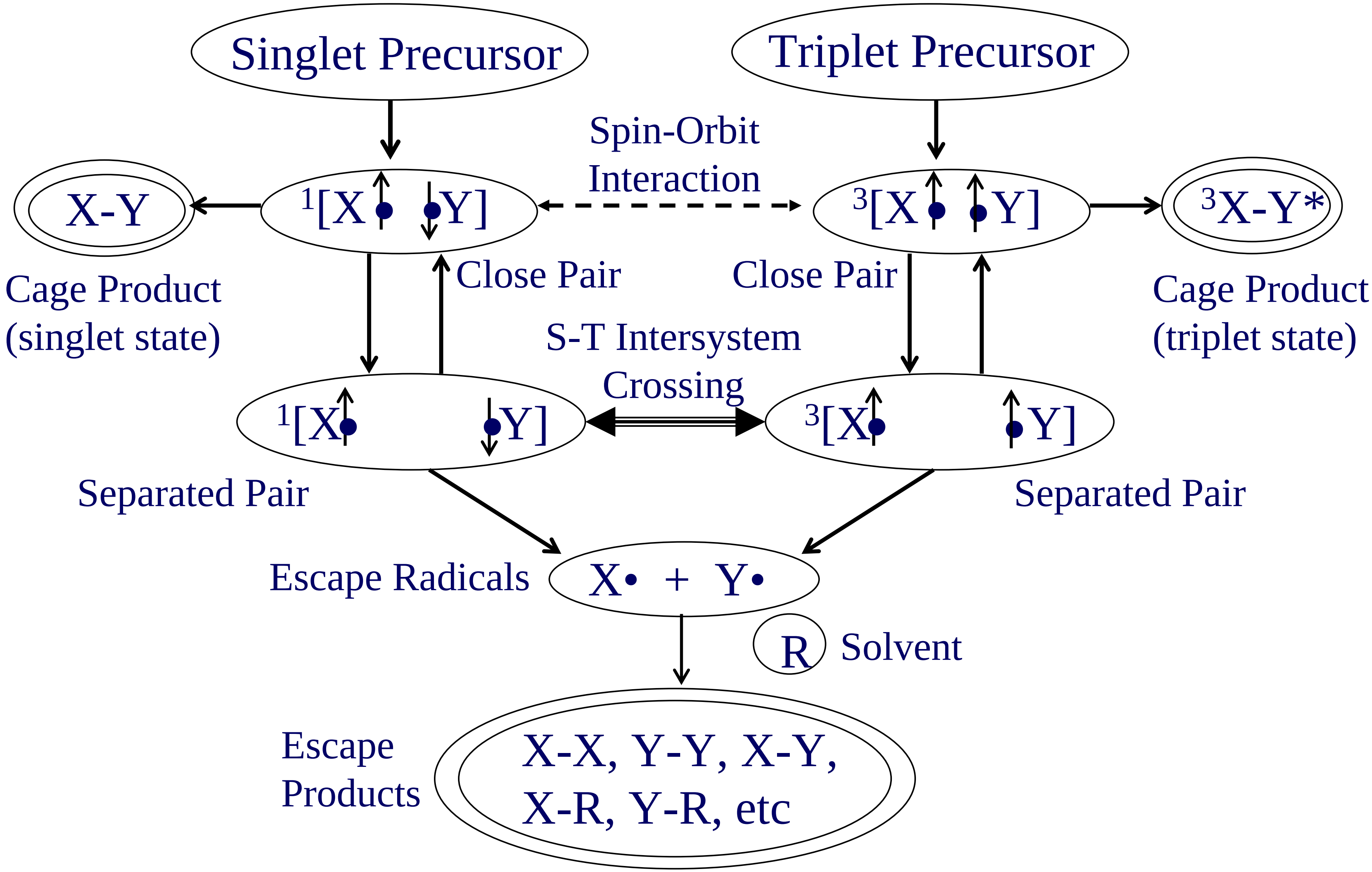

Reaction scheme of radical pairs generated from singlet and triplet precursors.
(Modified from Hayashi (2004))

Magnetic field effect in iron release: precipitation i

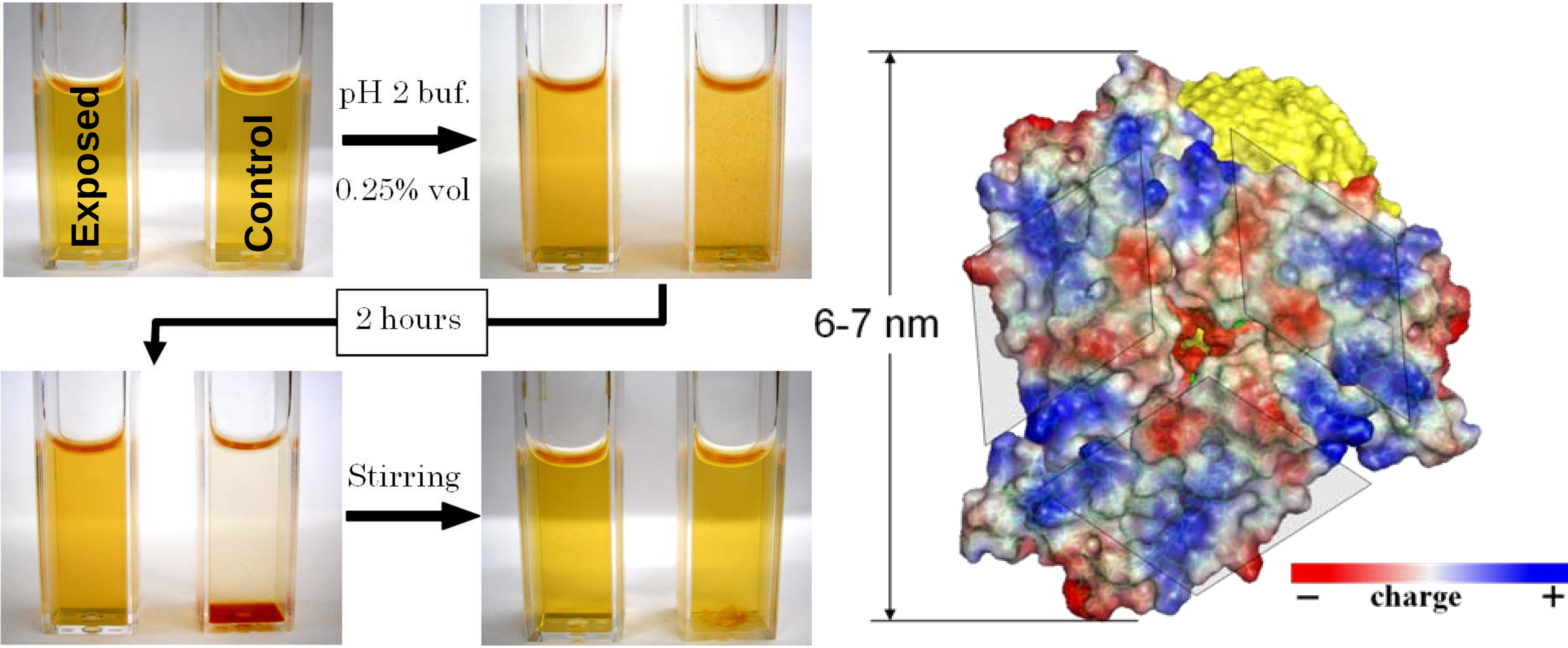

The 3-fold points act as hydrophilic terminals essential to protein solubility. A sudden release of iron via reducing agents leads to blocking of the terminals and protein aggregation, followed by precipitation. The effect is quenched in protein solutions exposed to magnetic fields

Protein functions: Iron absorption and release

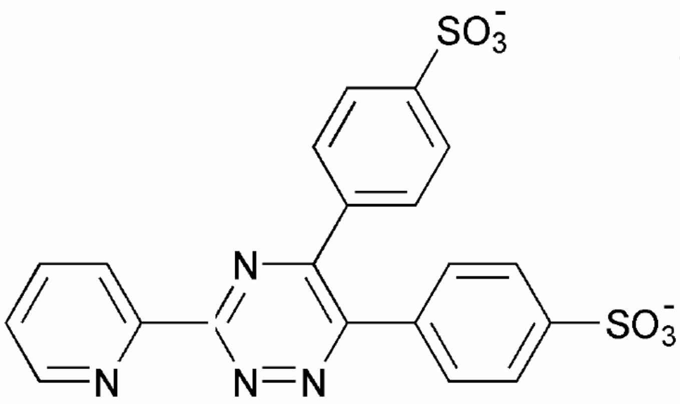

Guy N.L. Jameson et al., Org. Biomol. Chem. 2, 2346 (2004)

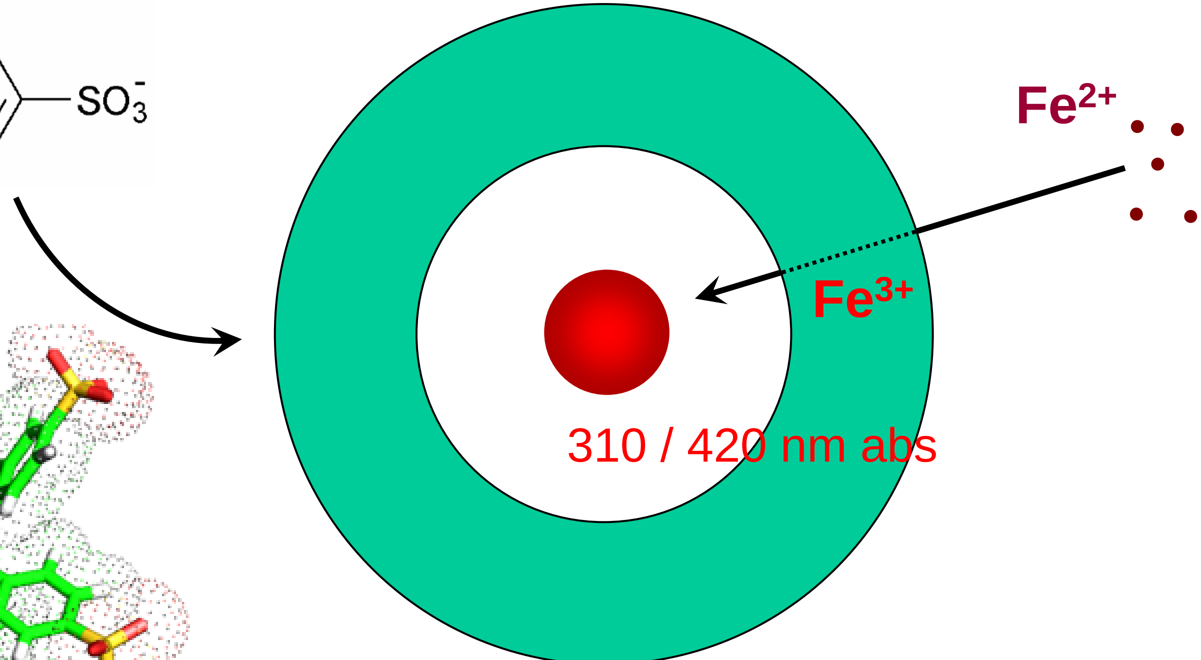

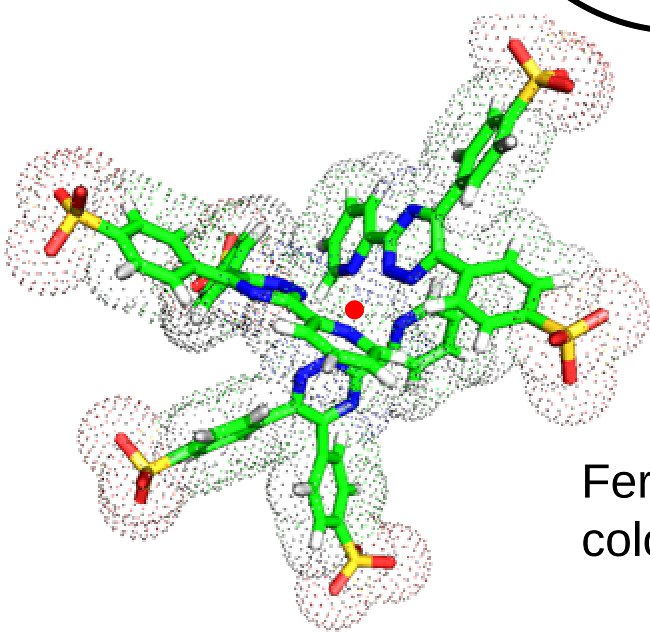

Ferrozine; iron chelator and
colorimetric probe (562 nm; ε = 29700 $M^{-1}cm^{-1}$)

Effects of RF magnetic fields on iron uptake and release vs. concentrations

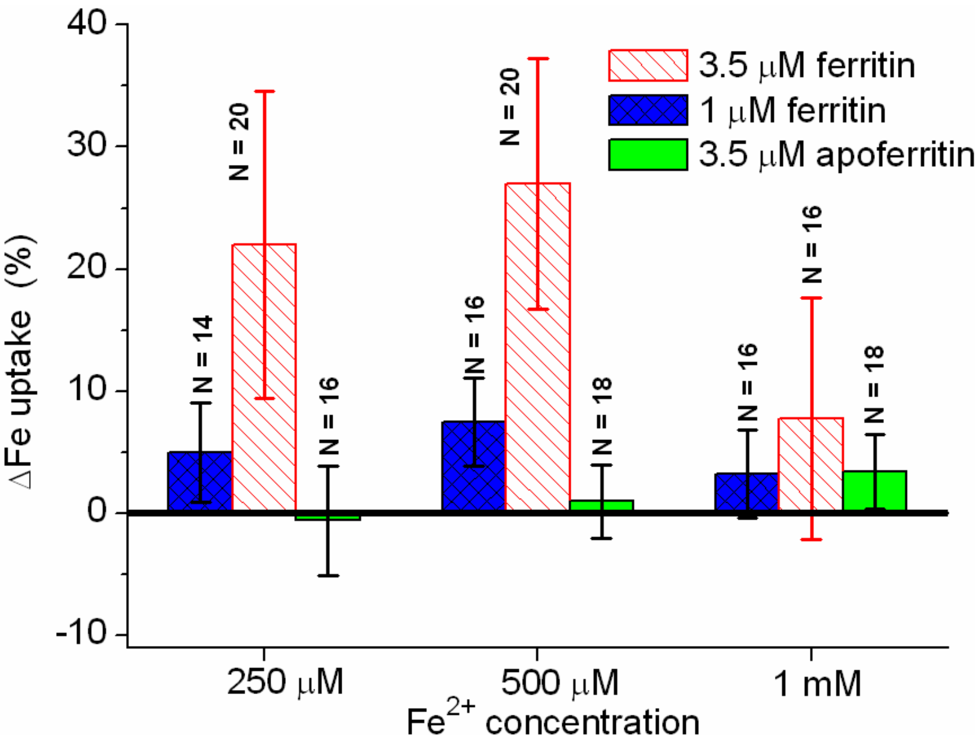

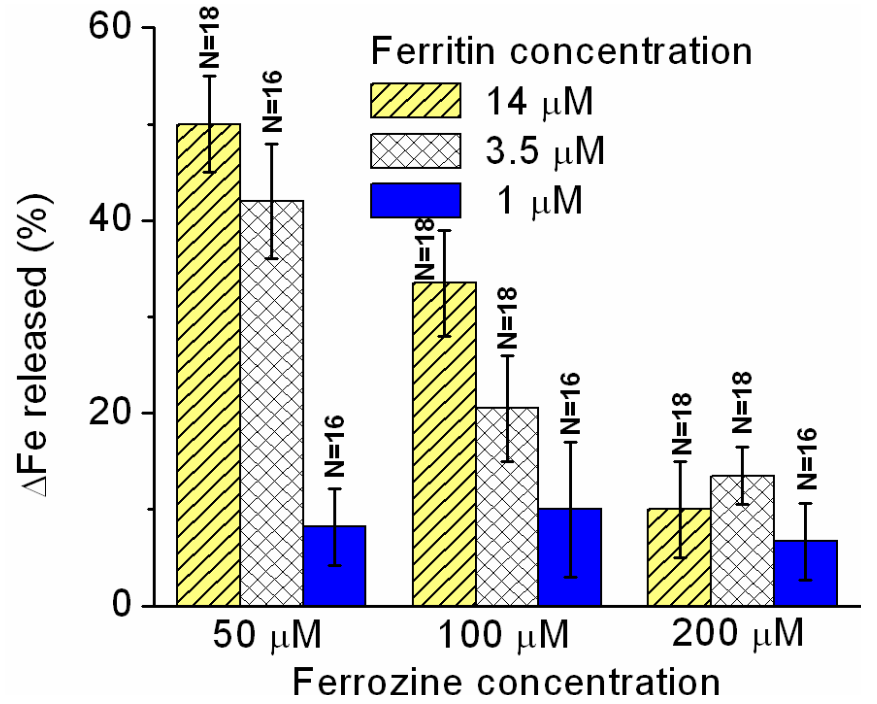

After a 5 hours exposure to fields of 1 MHz and 30 μT, the iron uptake and release are reduced. ΔFe uptake/released = (Fe $|_{control}$-Fe $|_{exposed}$) / Fe $|_{control}$, with Fe $|_{control}$ and Fe $|_{exposed}$ the iron chelated/uptaked after 1 hour in control and exposed samples, respectively.

O. Céspedes and S. Ueno, Bioelectromagnetics 30（2009)

1. TMS (Transcranial Magnetic Stimulation)

T. Tashiro, M. Fujiki, T. Matsuda, C. M. Epstin, M. Sekino, T. Maeno, H. Funamizu, M. Ogiue-Ikeda, K. Iramina, and S. Ueno

2. MEG (Magnetoencephalography)

K. Iramina, S. Iwaki, K. Gjini, T. R. Barbosa, and S. Ueno

3. Impedance/Conductivity MRI and Current MRI

M. Sekino, T. Matsumoto, T. Hatada, Y. Yukawa, N. Iriguchi, and S. Ueno

4. Cancer Therapy by Pulsed Magnetic Fields

M. Ogiue-Ikeda, S. Yamaguchi, Y. Sato, and S. Ueno

5. Cell Orientation and Growth by Magnetic Fields

M. Iwasaka, H. Kotani, Y. Eguchi, M. Ogiue-Ikeda, and S. Ueno

6. Ferritin and Iron Release/Uptake

O. Cespedes and S. Ueno